Tampere University

David Trejo Garcia

STABILITY OF (2+1)D SOLITONS IN THE GENERALLY NONLOCAL REGIME

Master of Science Thesis
Faculty of Engineering and Natural Sciences
Examiners: Prof. Marco Ornigotti
Prof. Andrea Marini
October 2021

ABSTRACT

David Trejo Garcia: Stability of (2+1)D solitons in the generally nonlocal regime
Master of Science Thesis
Tampere University
Photonics Technologies
October 2021

Since the description of accessible solitons by Snyder and Mitchel, the exploration of nonlocality in nonlinear media as a way to stabilize multidimensional solitons has received increasing attention. However, while the regimes of weak and strong nonlocality have been explored substantially, the case of general nonlocality remains scarcely investigated. This work seeks to explore this area, by testing the stability of (2+1)D beam profiles obtained through a perturbative approach, focusing on the generally nonlocal case of response functions of the Gaussian and exponential-decay types. The resulting semi-analytical expressions are perturbed LG modes, and their stability is tested under propagation using a split-step Fourier method. The simulations show that the beam profiles are very close to the exact soliton solutions within the generally nonlocal regime, which is an indication of the adequacy of the perturbative method to find soliton states. Both non OAM-carrying and OAM-carrying beams are explored. This work seeks to set a precedent for more detailed exploration of general nonlocality, which could provide advantages over simulation of other regimes, such as less computational costs.

Keywords: soliton, general nonlocality, orbital angular momentum, exponential-decay nonlocality, LG modes

PREFACE

I am very happy to have worked with solitons again, given that I have found them very appealing since I was first introduced to them. This time, I feel that certain concepts became more clear as I read through the literature. I hope that I was able to convey this in the description of what I did and the significance of my results. At the end of the day, I feel satisfied with my work and the knowledge and techniques that I have acquired.

This work would not have been possible without the help of my supervisors Marco Ornigotti and Charles Robson. Their patience and input in our weekly meetings were extremely valuable, not only for the development of this thesis, but for my career as a researcher as a whole. I hope we can continue working together in the future.

Of course, none of this would have been possible without the constant love and support of my family. Thank you to my parents and my brother for always supporting my crazy endeavours. Even though I left my country of Mexico for 2 years to pursue my master's degree, coming back home to them feels like I was never away.

To Diana, with whom I share the same thinking wavelength, I can only express immense gratitude for always being there for me across multiple countries and timelines. Let's start planning where in the space-time we'll meet again.

I am happy to have met such remarkable people during these 2 years, both inside and outside of the Europhotonics program. Thank you specially to Shroddha, Belquis, Jadon, Suvi, Shashank and Oumaïma for making my stay in both Marseille and Tampere so special and memorable.

Last but not least, thank you to Amélie Litman and Goery Genty, Coordinators of the Europhotonics program in France and Finland. I sincerely hope the program only keeps improving.

Tampere, 27th October 2021

David Trejo Garcia

CONTENTS

LIST OF SYMBOLS AND ABBREVIATIONS

${}_2F_1(a, b; c; z)$	Gaussian hypergeometric function
$\Gamma(x)$	Gamma function
$L_{km}(x)$	generalized Laguerre polynomial
LG mode	Laguerre Gaussian mode
NLS	Nonlinear Schrödinger equation
NNLS	Nonlocal Nonlinear Schrödinger equation
OAM	orbital angular momentum
TAU	Tampere University
TUNI	Tampere Universities
URL	Uniform Resource Locator

1. INTRODUCTION

As interest in nonlinear phenomena increased in the second half of the past century, so has the number of studies conducted around solitons. Since their first description by James Scott Russell in 1834 [1], notable effort has been put into understanding their inherent properties and interactions under all types of conditions.

Solitons are waves that conserve their shape along propagation. They have been observed in different branches of science, such as optics, biology, communication, fluid dynamics and Bose-Einstein condensates [1, 2]. The name "soliton" is meant to indicate that they interact like particles during collisions.

In the fields of optics and photonics, optical solitons refer to light beams confined during propagation. They are tightly related to solitary waves, and the terms are sometimes used without distinction in the context of photonics [1, 2, 3, 4]. The effects that allow the existence of optical solitons are a consequence of light propagating in nonlinear media. While linear media operates in a regime where the refractive index of the material does not change with intensity, nonlinear media introduces a intensity dependent variation in the refractive index [1].

Optical solitons can be classified as spatial or temporal. Spatial solitons are self-guided beams that remain confined in a direction transverse to propagation. This confinement is a result of a balancing between the natural tendency of a beam to diffract or spread and a self-focusing effect present in nonlinear media [1, 5]. Conversely, temporal solitons are pulses that keep their shape due to a balancing between self-phase modulation (SPM) and dispersion broadening. [1]. Extensive effort has been put into achieving these optical solitons experimentally [1, 2, 4, 6, 7, 8, 9, 10], as well as into finding adequate numerical and analytical models to describe them [5, 6, 7, 11, 12, 13, 14, 15, 16, 17, 18, 19, 20, 21, 22, 23, 24, 25, 26, 27].

Spatial optical solitons in (1+1)D (where the first "1" indicates the number of diffraction directions and the second "1" tells the direction of propagation) have been shown to be stable along propagation. However, multidimensional solitons in (2+1)D and (3+1)D are inherently unstable [18]. (2+1)D optical solitons usually suffer collapse over very short distances, which is a consequence of the self-focusing nature of a type of nonlinear media known as Kerr media. One of the first important achievements in understanding these

multidimensional solitons originated in what are now known as Townes solitons. These are analytical, theoretical solutions in the (2+1)D case, but they are unstable and collapse after a short, finite distance, which is why they have never been observed experimentally [13, 18, 28].

It has been suggested and proved that in order to stabilize (2+1)D solitons, either a potential or a medium with nonlocality can be used. For example, adding a harmonic oscillator potential allows to obtain stable numerical solutions within threshold values. These results have been summarized in a review by Malomed in [18].

Equally interesting is the history of exploiting the nonlocality of materials in order to stabilize multidimensional solitons. The work of Snyder and Mitchel [3] proved that collapse in (2+1)D solitons could be overcome in a medium with strong nonlocality. Since then, strong nonlocality has been used to describe an abundance of soliton families, for example [14, 22]. On the other hand, the case of weak nonlocality has also been explored thoroughly in BECs and plasmas, where solitons are also present [12].

Studies of solitons within the range of general nonlocality have been relatively scarce, compared to the cases of strong and weak nonlocality. Bang et al. [12] first proved rigorously that solitons could be stable in the generally nonlocal regime. Notably, Guo et al. [20] developed a method to examine the propagation of optical beams in sub-strong nonlocal media using a variational approach, and were able to obtain results very close to those predicted by the Snyder-Mitchel model. However, the approach by Guo requires the nonlocal response to be twice differentiable at the origin, which is seldom the case. Ouyang et al. [21] presented a model that is free from this limitation, as they approximate the refractive index of the material itself as a Taylor series. They are able to describe the propagation of solitons and periodic optical beams in generally nonlocal media for both Gaussian and exponential-decay nonlocal responses. This novel model is, however, only developed for the (1+1)D case and the results are relatively simple profiles.

The work of this thesis aims to further explore soliton behavior in the generally nonlocal case by extending the model by Ouyang to the (2+1)D case and characterize its solutions. Deng et al [22] have shown that, in the strongly nonlocal case, (2+1)D solitons in a symmetric nonlocal response correspond to a family of Laguerre Gaussian (LG) beams. Since the Ouyang model consists of adding a perturbation to the Hamltionian present in the strongly nonlocal case, the solutions in the generally nonlocal case are perturbed LG modes.

This thesis is organized as follows: Chapter 2 introduces all the theoretical framework necessary to understand the model of stabilization proposed in the following sections. Chapter 3 introduces a way to approximate solitons within a generally nonlocal regime. Chapter 4 tests the results obtained through methodology in Chapter 3. Finally, Chapter 5 discusses the results and presents some concluding remarks.

2. THEORETICAL FRAMEWORK

This chapter will introduce the concepts necessary to understand the methodology used to stabilize optical solitons and the results. More specifically, this chapter will:

- introduce the wave equation used to describe propagating electromagnetic waves,
- present the necessary approximations that lead to the equation known as the generalized nonlinear Schrödinger equation,
- introduce the shape of the variation of the refractive index as a function of the nonlocal response function, and
- explain the different degrees of nonlocality.

2.1 Optics in nonlinear media

Optical solitons exist as a consequence of light propagating in nonlinear media. In linear media, the induced polarization in a material has a linear relationship with the electric field [29], this is

$$P(t) = \chi^{(1)} E(t), \tag{2.1}$$

where $\mathbf{P}(\mathbf{r}, t)$ is the induced polarization, $\mathbf{E}(\mathbf{r}t)$ is the electric field and $\chi^{(1)}$ is known as the linear susceptibility. In this example, the vectorial nature of $P(t)$ and $E(t)$ has been ignored for simplicity.

As the name indicates, nonlinear materials do not follow this proportionality relationship. Instead, a common approach is to approximate the induced polarization as a power series of the electric field

$$P(t) = \chi^{(1)} E(t) + \chi^{(2)} E(t)^2 + \chi^{(3)} E(t)^3 + ..., \tag{2.2}$$

where $\chi^{(2)}$ and $\chi^{(3)}$ are the second order and third order susceptibilities, respectively.

When considering the vector nature of the induced polarization and the electric field, the linear susceptibility $\chi^{(1)}$ becomes a second-rank tensor, the second order susceptibility

$\chi^{(2)}$ becomes a third-rank tensor and so on [29]. The second order susceptibility can be neglected if the medium is assumed to have inversion symmetry [1]. More specifically, it can only occur in noncentrosymmetric crystals [29]. On the other hand, effects of the third order susceptibility $\chi^{(3)}$ can be observed in both centrosymmetric and noncentrosymmetric materials, so it is not neglected in this work.

A medium with predominantly a third order nonlinearity is called a Kerr medium [1, 2, 29].

2.2 Propagation of light in a nonlinear medium

From Maxwell's equations, it is possible to obtain an expression associated with the field propagating inside a medium [2]. This is

$$\nabla^2\mathbf{E} - \frac{1}{c^2}\frac{\partial^2\mathbf{E}}{\partial t^2} = \frac{1}{\epsilon_0 c^2}\frac{\partial^2\mathbf{P}}{\partial t^2}, \tag{2.3}$$

where c is the speed of light in vacuum and ϵ_0 is the electric permittivity of the medium. As established in the previous section, the induced polarization will have a linear and a nonlinear component, such that

$$\mathbf{P}(\mathbf{r},t) = \mathbf{P}_L(\mathbf{r},t) + \mathbf{P}_{\mathrm{NL}}(\mathbf{r},t), \tag{2.4}$$

where $\mathbf{P}_L(\mathbf{r},t)$ corresponds to the linear part of the polarization and $\mathbf{P}_{\mathrm{NL}}(\mathbf{r},t)$ corresponds to the nonlinear one. As mentioned before, when considering the vector nature of the induced polarization and the field, expressions become more complex than Eq. (2.1). For instance, the components of the polarization are expressed as

$$\mathbf{P}_L(\mathbf{r},t) = \epsilon_0 \int_{-\infty}^{\infty} \chi^{(1)}\left(t-t'\right)\cdot\mathbf{E}\left(\mathbf{r},t'\right)dt', \tag{2.5}$$

$$\begin{aligned}\mathbf{P}_{\mathrm{NL}}(\mathbf{r},t) =& \epsilon_0 \iiint_{-\infty}^{\infty} \chi^{(3)}\left(t-t_1,t-t_2,t-t_3\right) \\ &\times \mathbf{E}\left(\mathbf{r},t_1\right)\mathbf{E}\left(\mathbf{r},t_2\right)\mathbf{E}\left(\mathbf{r},t_3\right)dt_1dt_2dt_3.\end{aligned} \tag{2.6}$$

It is possible to simplify these expressions by assuming that the response of the medium is instantaneous. That way, the expression for the nonlocal component of the induced polarization is reduced to

$$\mathbf{P}_{\mathrm{NL}}(\mathbf{r},t) = \epsilon_0\chi^{(3)}\mathbf{E}(\mathbf{r},t)\mathbf{E}(\mathbf{r},t)\mathbf{E}(\mathbf{r},t). \tag{2.7}$$

The field can be assumed to be quasi-monochromatic [1]. Additionally, the nonlinear

induced polarization can be defined as a perturbation to $\mathbf{P}_L$ due to its lower magnitude [1, 29]. These assumptions lead to the following expression for the field

$$\mathbf{E}(\mathbf{r},t) = \frac{1}{2}\hat{x}\left[E(\mathbf{r},t)\exp\left(-i\omega_0 t\right) + \text{ c.c. }\right], \tag{2.8}$$

where ω_0 is the frequency of the field and it has assumed to be polarized in $\hat{x}$.

The nonlinear component of the polarization can be further simplified to

$$P_{\mathrm{NL}}(\mathbf{r},t) \approx \epsilon_0 \epsilon_{\mathrm{NL}} E(\mathbf{r},t), \tag{2.9}$$

where ϵ_{NL} is equal to:

$$\epsilon_{\mathrm{NL}} = \frac{3}{4}\chi^{(3)}_{xxxx}|E(\mathbf{r},t)|^2. \tag{2.10}$$

Here, $\chi^{(3)}_{xxxx}$ is one of the components of the third order susceptibility tensor $\chi^{(3)}$ of an isotropic material [29]. The material can be aligned so that this component is the only one that has an effect on the refractive index [1].

In analogy to the linear case, where the relative permittivity can be written in terms of the susceptibility [30] as $\epsilon_r = 1 + \chi_e$, the electric constant for the case of nonlinearity can be written as

$$\tilde{\epsilon}(\omega) = 1 + \chi^{(1)}_{xx}(\omega) + \epsilon_{\mathrm{NL}}, \tag{2.11}$$

where the tilde denotes a Fourier transform [1]. This leads to the possibility of expressing the refractive index as

$$\tilde{n}(\omega) = n_0 + n_2|E|^2, \tag{2.12}$$

where n_2 is related to the susceptibility tensor

$$n_2 = \frac{3}{8n}\,\mathrm{Re}\left(\chi^{(3)}_{xxxx}\right). \tag{2.13}$$

The importance of Eqs. (2.12) and (2.13) cannot be overstated: the description of dependence of the refractive index on the intensity $I = |E|^2$ is the basis for understanding phenomena such as four-wave mixing and third-harmonic generation [2].

2.3 Derivation of the nonlinear Schrödinger equation

In the context of solitons, several assumptions are made. The field is assumed to be in the paraxial approximation and linearly polarized. Also, it is assumed to propagate in the Z direction, hence it is expressed as $E(\mathbf{r}) = A(\mathbf{r})e^{(ik_0 n_0 Z)}$, where $A(\mathbf{r})$ is the envelope of the field amplitude, $k_0 = 2\pi/\lambda$ is the wavenumber and λ is the wavelength. Finally, since solitons are characterized by being localized, it is assumed that the field $\mathbf{E}(\mathbf{r}) \to 0$ as $r \to \infty$. Taking these considerations into account, propagation of a beam in a Kerr medium is determined by the following equation [1]:

$$2ik_0 n_0 \frac{\partial A}{\partial Z} + \left(\frac{\partial^2 A}{\partial X^2} + \frac{\partial^2 A}{\partial Y^2} \right) + 2k_0^2 n_0 n_2 |A|^2 A = 0. \tag{2.14}$$

Considering a beam with a waist of W_0, a change to dimensionless variables is possible:

$$x = X/W_0, \tag{2.15a}$$
$$y = Y/W_0, \tag{2.15b}$$
$$z = Z/L_d, \tag{2.15c}$$
$$u = (k_0|n_2|L_d)^{1/2} A, \tag{2.15d}$$

where $L_d = k_0 n_0 w_0^2$ is known as the Rayleigh length or Rayleigh range. Rewriting Eq. (2.14) in terms of these dimensionless variables:

$$i\frac{\partial u}{\partial z} + \frac{1}{2}\frac{\partial^2 u}{\partial x^2} + \frac{1}{2}\frac{\partial^2 u}{\partial y^2} \pm |u|^2 u = 0. \tag{2.16}$$

Eq. 2.16 is usually referred to as the nonlinear Schrödinger (NLS) equation.

2.4 The nonlocal nonlinear Schrödinger equation

The model described by (2.16) assumes that the response of the medium is local, meaning that the field at a certain point depends exclusively on the intensity at that point. As it was mentioned in the Introduction, there is a motivation to consider the effect of nonlocality in Kerr media, since it could potentially stabilize solitons that would otherwise suffer collapse [12].

The properties of a beam propagating in nonlocal media depend on the intensity of an area surrounding the point of interest [26]. Nonlocality is naturally present in systems like nematic liquid crystals and photorefractive materials [3]. Solitons have been shown to interact differently in nonlocal media [3, 31]. It is possible to generalize Eq. (2.16) by

considering the effects of nonlocality [16] :

$$i\frac{\partial u}{\partial z} + \frac{1}{2}\frac{\partial^2 u}{\partial x^2} + \frac{1}{2}\frac{\partial^2 u}{\partial y^2} \pm N(|u|)u = 0, \tag{2.17}$$

with $N(|u|)$ being equal to [16]

$$N(|u|) = \int_{-\infty}^{\infty}\int_{-\infty}^{\infty} R(\mathbf{r}-\mathbf{r}')|u(\mathbf{r}',z)|^2 d^2\mathbf{r}'. \tag{2.18}$$

Eq. (2.17) is known as the nonlocal nonlinear Schrödinger equation (NNLS) and $R(\mathbf{r})$ is known as the nonlocal response function or nonlocal kernel of the system.

2.5 The nonlocal response function and the degree of nonlocality

As mentioned in the past sections and the Introduction, the nonlocal response function, or nonlocal kernel $R(\mathbf{r})$, is an indicator of the extension of the nonlocal effects in the system [16, 26].

One of the most important concepts when talking about the nonlocal response is the degree of nonlocality. Usually, it is defined as the ratio between the width of nonlocal response, defined with ω_0, and the width of the soliton μ [21]. It is worth mentioning, however, that there are some authors that defining as the inverse of that [22]. In this work, the first definition will be the one used.

Depending on the value of the degree of nonlocality, several nonlocal cases are usually defined. Naturally, when the response function is equal to a Dirac delta function $\delta(\mathbf{r})$, the local case is retrieved and Eq. (2.17) reduces to Eq. (2.16). If the width of the response function is finite but comparatively smaller than the width of the soliton, this corresponds to the case of weak nonlocality. IF the width of the nonlocality is comparable to the width of the soliton, then the case is the generally nonlocal. Finally, if the width of the nonlocality is much larger than the width of the soliton, it is said that it is the case of strong nonolocality. Fig. 2.1 exemplifies these cases.

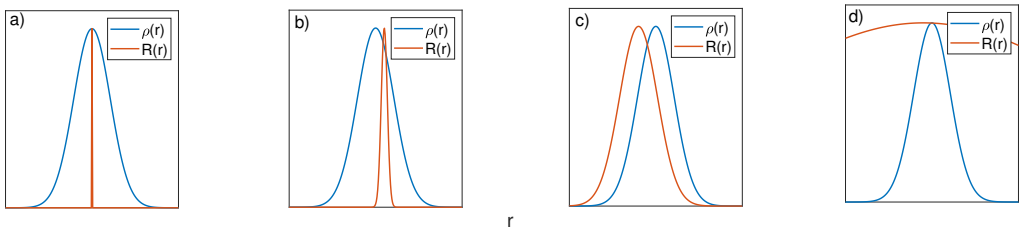

Figure 2.1. *A visual representation of a) local, b) weakly nonlocal, c) generally nonlocal and d) strongly nonlocal cases. In all figures, $\rho(r)$ represents the soliton profile and $R(r)$ is the response function. It is important to mention that all functions have been scaled to have the same amplitude, which in practice is not necessarily the case. The offset of $R(r)$ in b), c) and d) is a reminder that the nonlocal response is convoluted with the beam profile in Cartesian coordinates.*

Two of the most studied models of nonlocality are the gaussian and exponential-decay cases [5, 21, 26, 32].

Gaussian nonlocality has not been observed in nature. However, it is often explored due to its smooth behavior and ease to work with. On the other hand, exponential decay nonlocality is present in nematic liquid crystals [7, 10, 21].

3. METHODOLOGY

Now that the model to describe nonlocal solitons has been stated in the form of Eqs. (2.17) and (2.18), this chapter aims to find analytical or semi-analytical solutions to it.

The method used in this chapter is similar to the one used by Ouyang et al. in [21], but it is extended to the case of (2+1)D and cylindrical coordinates, and it is explained in its entirety in Chapter 3.1 As a summary, the methodology consists of:

- shifting to the more natural case of cylindrical coordinates,
- proposing an Ansatz to the model based on it is known from [21] and [22],
- approximating the nonlocal nonlinear element of the model as a linear Taylor series, and
- solving the linear model using perturbation theory.

Sections 3.2 and 3.3 correspond to applying this methodology to non-OAM and OAM carrying beams, respectively.

3.1 Semi-analytical solution to the NNLSE

The types of nonlocal responses analyzed in this work are all radially symmetric, which means that $R(\vec{r})$ depends only on the radial coordinate r, where $r^2 = x^2 + y^2$. This makes the cylindrical coordinate system a more natural choice to describe the Eqs. (2.17) and (2.18), which transform in the following way:

$$i\frac{\partial u}{\partial z} + \frac{1}{2}\left(\frac{\partial^2 u}{\partial r^2} + \frac{1}{r}\frac{\partial u}{\partial r} + \frac{1}{r^2}\frac{\partial^2 u}{\partial \theta^2}\right) + u\int_0^{2\pi}\int_0^{\infty} R(r-\xi)|u(\xi,\theta,z)|^2 \xi d\xi d\theta = 0. \quad (3.1)$$

Eq. (3.1) is now expressed in the cylindrical coordinate system and the integration limits have been adequately changed. The solution u will propagate in the z direction and diffract in the x and y directions, or the r direction in the case of cylindrical coordinates. It is natural to assume that u is in fact a product of three independent functions, each depending on a single variable. This method is called separation of variables and is used

extensively in solving partial differential equations [33, 34]. This leads to the Ansatz

$$u(r,\theta,z) = \rho(r)\Theta(\theta)e^{-i\gamma z}, \tag{3.2}$$

where the term γ is a propagation constant. Before substituting this Ansatz in Eq. (3.1), the nonlocal nonlinear part can be defined separately as

$$V(r) = -\int_0^{2\pi}\int_0^{\infty} R(r-\xi)|u(\xi,\theta,z)|^2 \xi d\xi d\theta, \tag{3.3}$$

where $V(r)$ depends only on r, due to integration in $theta$. Substitution of Eqs. (3.2) and (3.3) into Eq. (3.1) leads to the solution to the angular part

$$\gamma\rho(r)\Theta(\theta) + \frac{1}{2}\left(\frac{\partial^2}{\partial r^2} + \frac{1}{r}\frac{\partial}{\partial r} + \frac{1}{r^2}\frac{\partial}{\partial \theta^2}\right)\rho(r)\Theta(\theta) - \rho(r)\Theta(\theta)V(r) = 0. \tag{3.4}$$

Eq. (3.4) can be separated into two independent radial (r dependent) and angular (θ dependent) parts that need to be equal, which is only possible if both are equivalent to a constant. Solving the angular part with this method results in the expression

$$\Theta(\theta) = \frac{1}{\sqrt{2\pi}}e^{i\theta m}, \tag{3.5}$$

which has been normalized so that $\int_0^{2\pi}\Theta(\theta)d\theta = 1$. The term m in beams with an angular dependence such as Eq. (3.5) is called the topological charge [1]. Moreover, beams with $m \neq 0$ are said to carry nonzero orbital angular momentum (OAM) [35, 36]. Deng et al. [22] have also studied the case of a (2+1)D nonlocal response function with radial symmetry, although they focus on the strongly nonlocal case. Since their result yields a family of Laguerre-Gaussian (LG) beams, it is safe to assume that the solutions to this model will be functions similar to LG beams. These functions have the property of radial symmetry around $r = 0$, similarly to the nonlocal response functions that are being considered. Because of this, it is appropriate to make a Taylor expansion of Eq. (3.3) around this point

$$V(r) = V(0) + \frac{V^{(2)}(0)}{2!}r^2 + \frac{V^{(4)}(0)}{4!}r^4 + \frac{V^{(6)}(0)}{6!}r^6 + ..., \tag{3.6}$$

where the odd parts of the expansion are equal to zero due to the symmetry of the response function [37]. For convenience, Eq. (3.6) can be redefined in terms of new con-

stants

$$V(r) = V_0 + \frac{1}{2\mu^4} r^2 + \alpha r^4 + \beta r^6, \tag{3.7}$$

with each new term being defined as

$$V_0 = V(0), \tag{3.8a}$$
$$\frac{1}{\mu^4} = V^{(2)}(0), \tag{3.8b}$$
$$\alpha = \frac{1}{4!} V^{(4)}(0), \tag{3.8c}$$
$$\beta = \frac{1}{6!} V^{(6)}(0). \tag{3.8d}$$

By substituting Eq. (3.5) and Eq. (3.7) in Eq. (3.4), and setting the propagation constant $\gamma = \varepsilon - V_0$, the resulting expression (where the dependence on r of ρ has been omitted for simplicity) is

$$\left[-\frac{1}{2}\frac{d^2}{dr^2} - \frac{1}{2r}\frac{d}{dr} + \frac{m^2}{2r^2} + \frac{1}{2\mu^4} r^2 + \alpha r^4 + \beta r^6 \right] \rho = \varepsilon \rho, \tag{3.9}$$

where ε is the energy associated with the solution. Eq. (3.9) has the form of a Schrödinger equation. The case $\alpha = \beta = 0$ corresponds to the harmonic oscillator in cylindrical coordinates [38], which makes Eq. (3.9) the Schrödinger equation for a harmonic oscillator with perturbation parameters α and β.

The reason r^8 and higher orders are not considered is because this work will mainly deal with solutions in the generally nonlocal and highly nonlocal regimes, therefore when $r < \mu$, the terms αr^4 and βr^6 are several orders of magnitude smaller than $\frac{1}{\mu^4} r^2$, which is indicative that the r^8 and the following terms are even less significant to the full effect or $V(r)$, and are therefore neglected.

The case of a Schrödinger equation with a perturbed harmonic oscillator hamiltonian has been widely studied in fields such as quantum mechanics and optics [21, 33, 34]. Solving it requires to know the unperturbed solution first, followed by use of perturbation theory. Appendix A shows how to get the answer to the unperturbed case of Eq. (3.9), in which $\alpha = \beta = 0$. This results in

$$\rho^{(0)}_{km}(r) = \sqrt{\frac{2k!}{\mu^2 \Gamma(m+k+1)}} \left(\frac{r^2}{\mu^2} \right)^{\frac{|m|}{2}} e^{-\frac{r^2}{2\mu^2}} L_{km}\left(\frac{r^2}{\mu^2} \right), \tag{3.10}$$

where $L_{km}(x)$ is the generalized Laguerre polynomial, k is the order of the polynomial. More properties about Laguerre polynomials can be reviewed in most books for mathematical methods in physics, for example [39]. The value of k is related to the soliton energy by $k = \frac{1}{2}(\varepsilon\mu^2 - m - 1)$, which means that the unperturbed energy is

$$\varepsilon_{km}^{(0)} = \frac{2k + m + 1}{\mu^2}, \tag{3.11}$$

where the (0) superindex in both (3.10) and (3.11) indicates that these are the unperturbed solutions.

3.2 Non OAM-carrying beam

With the unperturbed radial expression given by Eq. (3.10), it is possible to obtain solutions to Eq. (3.9) using non-degenerate perturbation theory [33, 34]. This allows to have solutions of the form

$$u_{km}(r, \theta, z) = \frac{1}{\sqrt{2\pi}}\rho_{km}(r)e^{i\theta m}e^{-i(\varepsilon+V_0)z}. \tag{3.12}$$

where $\rho_{km}(r)$ are the radial solutions obtained with perturbation theory, as indicated by the lack of the (0) superindex compared to Eq. (3.10).

Naturally, Eq. (3.9) will have a family of solutions for different values of k and m. The simplest solution is the one with values $k = 0, m = 0$. In this work, this solution will be referred to as the non OAM-carrying beam ρ_{00}. It is also called the fundamental solution in the literature [1].

Appendix B shows how to obtain ρ_{00} from (3.9) using second order nondegenerate perturbation theory. This leads to

$$\begin{aligned}
\rho_{00} =& \frac{\sqrt{2}}{\mu}Ae^{-\frac{r^2}{2\mu^2}}\left[1 + \alpha\left(3\mu^4 - 2\mu^2r^2 - \frac{r^4}{2}\right)\right. \\
&+\beta\left(11\mu^6 - 6\mu^4r^2 - \frac{3\mu^2}{2}r^4 - \frac{1}{3}r^6\right) \\
&+\alpha\beta\left(-\frac{95\mu^{10}}{3} - 40\mu^8r^2 - 4\mu^6r^4 - \frac{2\mu^4r^6}{9}\right) \\
&+\alpha^2\left(-\frac{3\mu^8}{2} - 6\mu^6r^2 - \frac{\mu^4}{2}r^4\right) \\
&\left.+\ \beta^2\left(-\frac{239\mu^{12}}{2} - 66\mu^{10}r^2 - \frac{15\mu^8}{2}r^4 - \frac{2\mu^6}{3}r^6\right)\right],
\end{aligned} \tag{3.13}$$

where A is a soliton amplitude parameter. Naturally, setting $\alpha = \beta = 0$ recovers the solution to the unperturbed case. The energy associated to this beam can also be calculated using perturbation theory. It corresponds to

$$\varepsilon_{00}(r) = \frac{1}{\mu^2} + 4\alpha\mu^2 - 36\sqrt{2}\alpha^2\mu^5 + 6\beta\mu^6 - 360\sqrt{2}\alpha\beta\mu^7 - 996\sqrt{2}\beta^2\mu^9. \tag{3.14}$$

3.3 OAM carrying beam

Similarly to the previous section, a perturbed solution to Eq. (3.9) with values $k = 0, m = 1$ is obtained in Appendix C. This solution is referred to as in this work as the OAM-carrying beam ρ_{01}. This comes from the nonzero value of m in Eq. (3.12).

The solution worked in Appendix C is

$$\begin{aligned}\rho_{01}(r) =& \frac{\sqrt{2}}{\mu} A e^{-\frac{r^2}{2\mu^2}} \sqrt{\frac{r^2}{\mu^2}} \left[1 + \alpha\left(9\mu^4 - 3\mu^2 r^2 - \frac{1}{2}r^4\right)\right. \\ &+\beta\left(44\mu^6 - 12\mu^4 r^2 - 2\mu^2 r^4 - \frac{1}{3}r^6\right) \\ &+\alpha\beta\left(124\mu^{10} - 240\mu^8 r^2 - 16\mu^6 r^4 - \frac{2\mu^4}{3}r^6\right) \\ &+\alpha^2\left(\frac{51\mu^8}{2} - 27\mu^6 r^2 - \frac{3\mu^4}{2}\right) \\ &\left.+\ \beta^2\left(-160\mu^{12} - 528\mu^{10} r^2 - 40\mu^8 r^4 - \frac{8\mu^6}{3}r^6\right)\right].\end{aligned} \tag{3.15}$$

where the radial part is included in the term $e^{i\theta m}$.

The energy associated to this function is:

$$\varepsilon_{01} = \frac{2}{\mu^2} + 12\alpha\mu^2 - 156\sqrt{2}\alpha^2\mu^5 + 24\beta\mu^6 - 2016\sqrt{2}\alpha\beta\mu^7 - 7008\sqrt{2}\beta^2\mu^9 \tag{3.16}$$

This solution is also an example of a vortex beam [1, 35, 36], which correspond to beams having a topological charge $m \neq 0$. Vortex beams and solitons are characterized by a point of zero amplitude at the origin [1].

Up to this point, both Eqs. (3.13) and (3.15) are independent of the type of nonlocal response function $R(r)$. In the following chapter, the Gaussian nonlocality and the

exponential-decay nonlocality models are analyzed and values for coefficients A, α, and β are approximately obtained.

4. RESULTS

The aim of this Chapter is to prove the adequacy of the non-OAM carrying $(m = 0)$ beam ρ_{00}, shown in Eq (3.13), and the OAM carrying $(m = 1)$ beam ρ_{01}, shown in Eq. (3.15), as solutions to the NNLS, Eqs. (2.17) and (2.18).

The process to obtain ρ_{00} and ρ_{01} in Chapter 3 is independent of the shape of the nonlocal response function, as long as it is radially symmetric. This Chapter will then show these beams propagating in media with Gaussian and exponential-decay nonlocalities. As mentioned in Chapter 1, these are two of the most widely studied and used models of nonlocality. Examples of both the generally nonlocal and strongly nonlocal cases will be presented.

4.1 Propagation in media with Gaussian nonlocality

The model for Gaussian nonlocality is represented by [26, 32]

$$R(r) = \frac{1}{\pi\omega_0^2} e^{-\frac{r^2}{\omega_0^2}}, \tag{4.1}$$

where ω_0 is the width of the nonlocal response function. This expression has been normalized, so that $\int_0^{2\pi}\int_0^{\infty} R(r) r dr d\theta = 1$, which is a necessary condition for a nonlocal response function [26]. Fig. 4.1 shows the effect of the parameter ω_0.

Obtaining values for parameters A, V_0, α, β and μ in Eqs. (3.13) and (3.15) for a given value of ω_0 will define the system entirely. Notably, the last three Eqs. from (3.8) form a system of equations with four unknown values, A, μ, α and β (since the value V_0 does not appear in the definitions of (3.13) or (3.15)). This is significant because fixing one of these quantities will determine the other three. By selecting $\mu = 1$, the rest of the coefficients can be obtained for a given width of the nonlocal response function ω_0. μ is chosen to be 1 in order to keep the computations simple and the simulation window small.

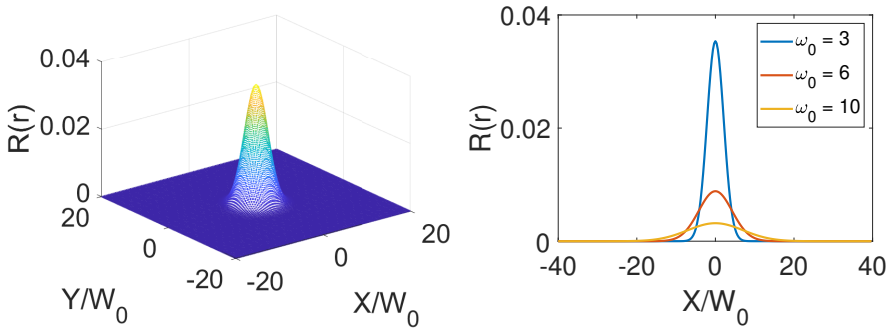

Figure 4.1. *Representation of a Gaussian nonlocal response function. The figure shows a) the 3D profile for* $\omega_0 = 3$ *and b) a 2D profile along* $Y/W_0 = 0$ *for different values of* ω_0*. The constraint imposed by the normalization condition has an effect on the magnitude of* $R(r)$*.*

4.1.1 Non OAM-carrying beam

Due to the relative complexity of the Eq. (3.3) after substitution of (4.1) and (3.13), it can be quite time consuming to obtain A, α and β analytically. Instead, a numerical fixed point method is used. Basically, this method approaches the correct values from a seed value until convergence is reached. The process is further detailed in Appendix D.

Table 4.1 shows the beam parameters calculated for different values of ω_0. These particular values were chosen to get a complete picture of how the degree of nonlocality affects the quality of the soliton solution within the generally nonlocal and strongly nonlocal regimes. Distinctly, a significant growth in the amplitude parameter A is observed as the degree of nonlocality is increased, which is consistent with studies of nonlocal solitons [5].

Table 4.1. *Beam parameters of* ρ_{00} *for* $\mu = 1$ *and several values of* ω_0*. Both* $\omega_0 = 3$ *and* $\omega_0 = 6$ *correspond to the generally nonlocal case and* $\omega_0 = 10$ *describes the strongly nonlocal case.*

	$\omega_0 = 3$	$\omega_0 = 6$	$\omega_0 = 10$
A	12.7632	46.4467	126.6170
α	-0.0245	-0.0067	-0.0025
β	8.0021×10^{-4}	6.0581×10^{-5}	8.1601×10^{-6}

After defining the values of the parameters, each profile is numerically propagated to observe its stability. To do this, a simulation is done with a split-step Fourier method with a step size equal to $dz = 0.2$. Figs. 4.2, 4.3 and 4.4 show the results of these propagations, each one for a different value of the degree of nonlocality. Going back to the definition of degree on nonlocality in Chapter 1, the cases $\omega_0/\mu = 3$ and $\omega_0/\mu = 6$ correspond to the generally nonlocal case, while $\omega_0/\mu = 10$ belongs to the strongly nonlocal case. Each

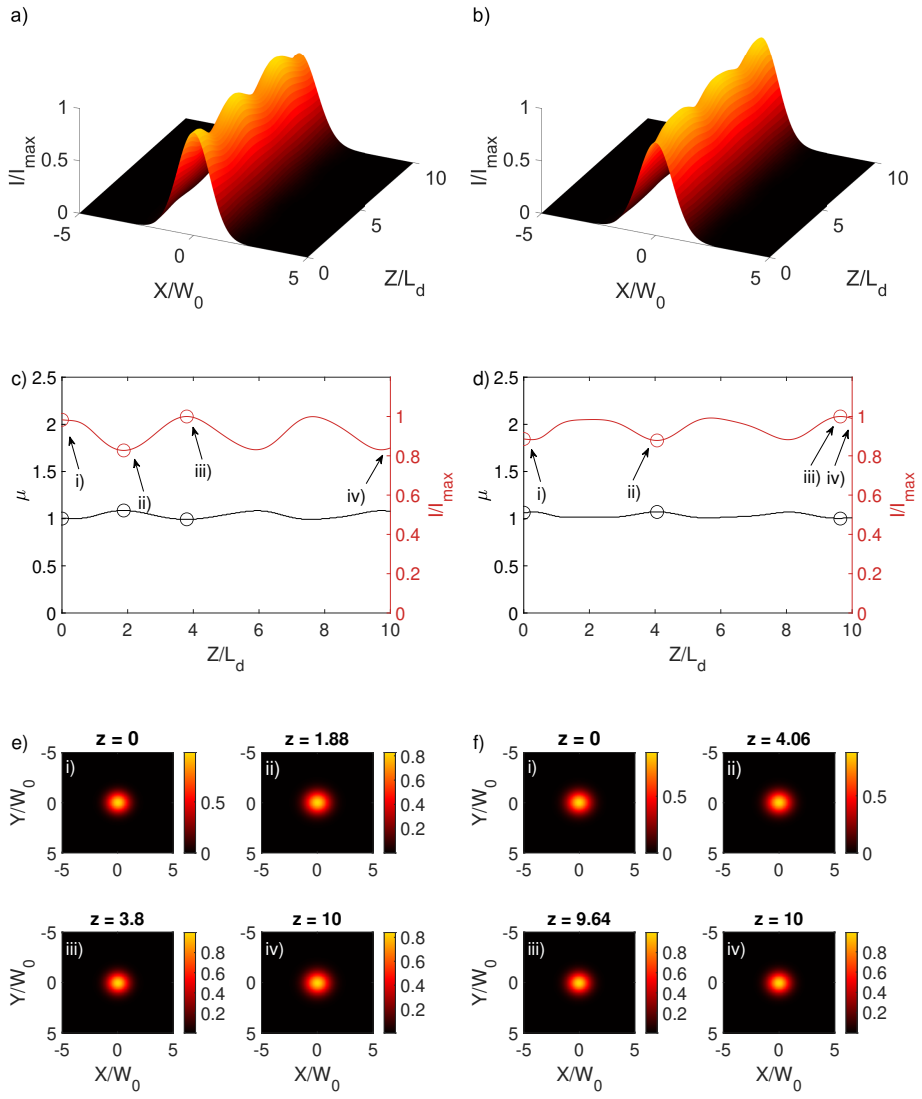

Figure 4.2. *Propagation of* ρ_{00} *with parameters* $A = 12.7632, \alpha = -0.0245, \beta = 8.0021 \times 10^{-4}$ *(left column) and* $A = 12.7632, \alpha = 0, \beta = 0$ *(right column), corresponding to the* 0^{th} *and* 2^{nd} *order approximations, respectively. The degree of nonlocality is* $\omega_0/\mu = 3$*. Figs. a) and b) show the propagation along* Z/L_D *for* $Y/W_0 = 0$*, c) and d) show the variation of normalized intensity and width, and e) and f) show the transverse profile at i) the input, ii) the minimum value of intensity, iii) the maximum value of intensity and iv) the output.* I_max *is equal to 52.7316 for the* 0^{th} *order and 51.1871 for the* 2^{nd} *order.*

figure consists of two columns: the left one shows the 0^{th} order approximation and the right one corresponds to the 2^{nd} order approximation.

Fig. 4.2 shows the result of the propagation for a degree of nonlocality of $\omega_0/\mu = 3$. While the beam is shown to propagate a distance of $Z/L_d = 10$ whitout collapse, several oscillations along propagation are observed. These have been identified before in numerical propagation of (2+1)D solitons, for example in [5], and are primarily attributed to excitations of the modes different than the soliton mode [1]. Fig. 4.2 also shows a

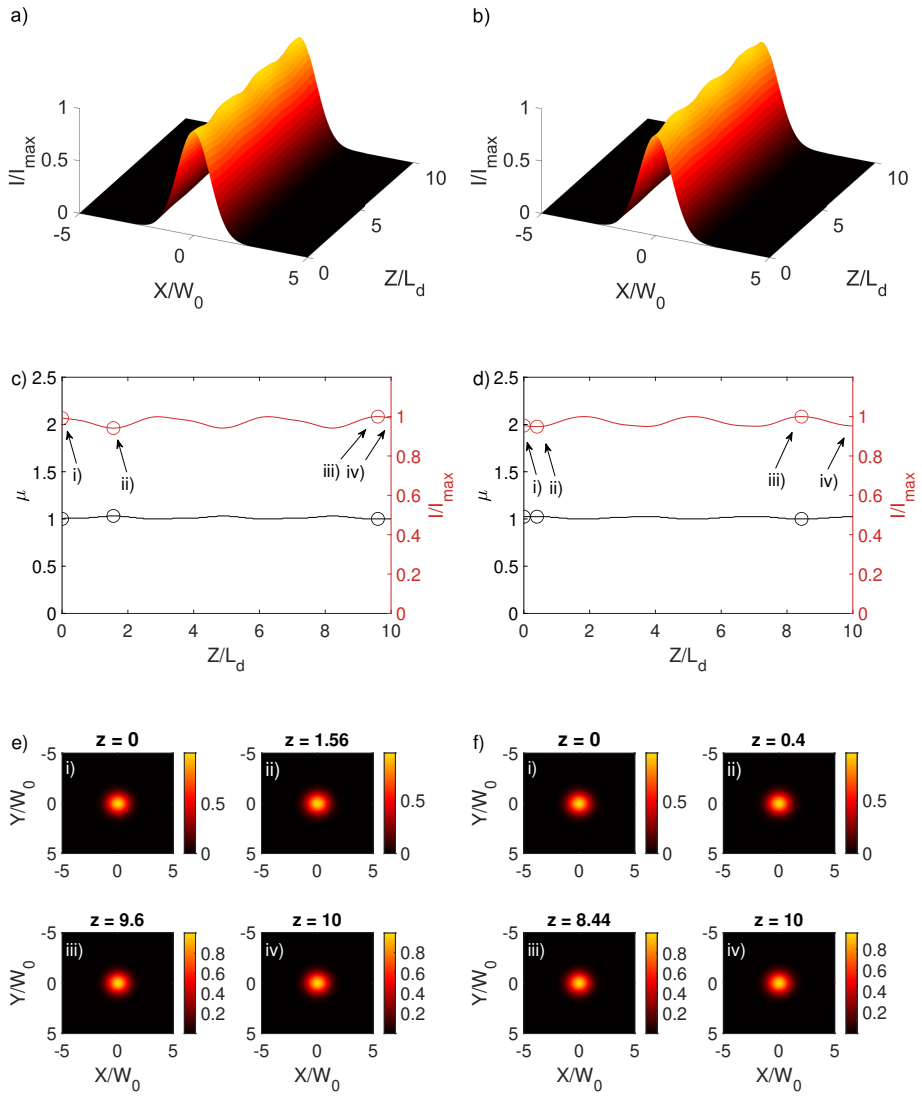

Figure 4.3. *Propagation of ρ_{00} with parameters $A = 46.4467, \alpha = -0.0067, \beta = 6.0581 \times 10^{-5}$ (left column) and $A = 46.4467, \alpha = 0, \beta = 0$ (right column), corresponding to the 0^{th} and 2^{nd} order approximations, respectively. The degree of nonlocality is $\omega_0/\mu = 6$. Figs. a) and b) show the propagation along Z/L_D for $Y/W_0 = 0$, c) and d) show the variation of normalized intensity and width, and e) and f) show the transverse profile at i) the input, ii) the minimum value of intensity, iii) the maximum value of intensity and iv) the output. I_max is equal to 692.0383 for the 0^{th} order and 691.7355 for the 2^{nd} order.*

variation of 15.8641% of the intensity for the 0^{th} order and a variation of 12.9324% for the 2^{nd} order, while the numerical width varies 8.5603% and 5.8608% respectively.

Similarly, Fig. 4.3 describes ρ_{00} in the case of $\omega_0/\mu = 6$, with the degree of nonlocality being higher but still within the regime of general nonlocality. For this case, the variation of intensity is only 5.0893% for the 0^{th} order and 4.7795% for the 2^{nd} order, while the width varies 3.1128% and 2.2814% respectively. It is also worth noting that the gap between the 0^{th} and 2^{nd} order approximations has been reduced.

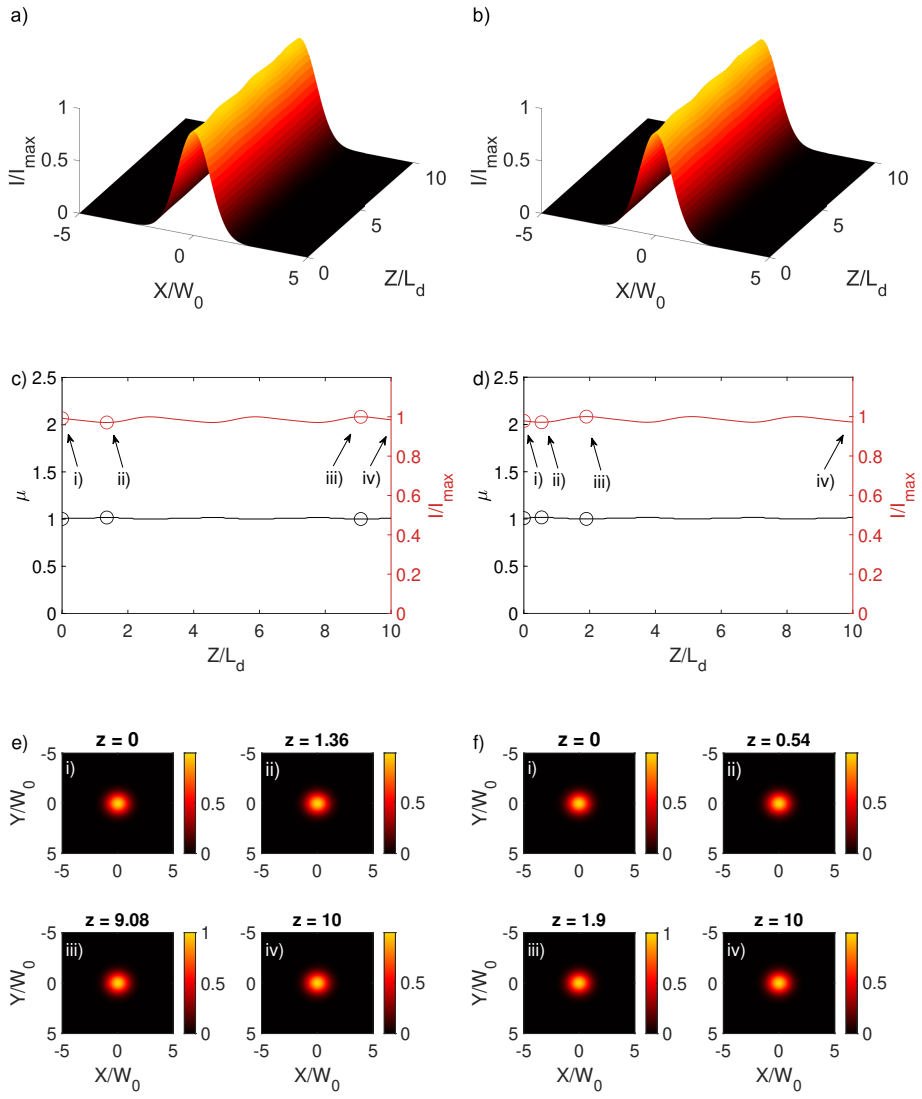

Figure 4.4. *Propagation of* ρ_{00} *with parameters* $A = 126.6170, \alpha = -0.0025, \beta = 8.1601 \times 10^{-6}$ *(left column) and* $A = 126.6170, \alpha = 0, \beta = 0$ *(right column), corresponding to the* 0^{th} *and* 2^{nd} *order approximations, respectively. The degree of nonlocality is* $\omega_0/\mu = 10$*. Figs. a) and b) show the propagation along* Z/L_D *for* $Y/W_0 = 0$*, c) and d) show the variation of normalized intensity and width, and e) and f) show the transverse profile at i) the input, ii) the minimum value of intensity, iii) the maximum value of intensity and iv) the output.*I_max *is equal to 5142.0049 for the* 0^{th} *order and 5138.8303 for the* 2^{nd} *order.*

Finally, Fig. 4.4 shows the case $\omega_0/\mu = 10$, which is already in the strongly nonlocal regime. The maximum variation in intensity with respect to the input is 2.1549% for the 0^{th} order and 2.2111% for the 2^{nd} order, while the width varies 1.5564% and 0.7722% respectively.

4.1.2 OAM-carrying beam

The methodology of the fixed point method described in the previous section and Appendix D is used in conjuction with expression (3.15), in order coefficients for the OAM-carrying beam. Natuarrly, the response function is still the one described by the Gaussian expression in (4.1). The results are reported in Table 4.2.

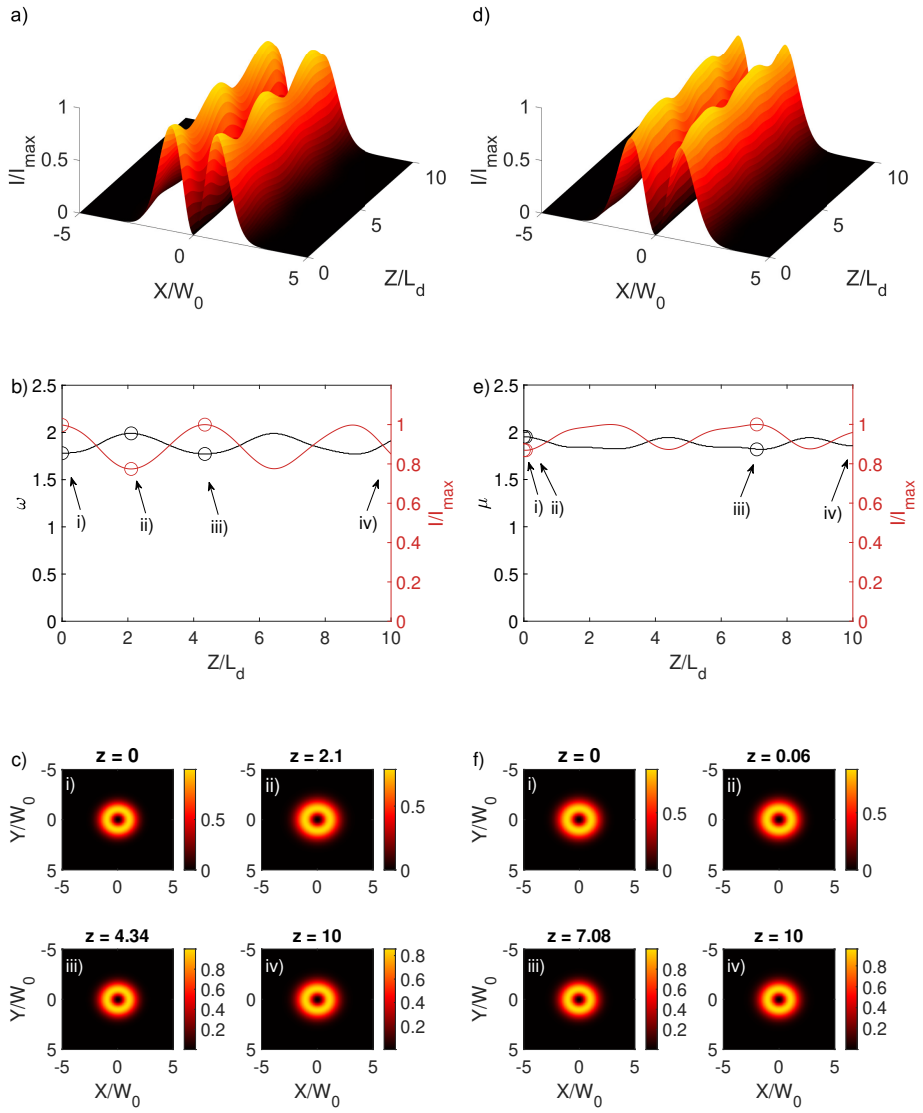

Figure 4.5. *Propagation of* ρ_{01} *with parameters* $A = 14.6804, \alpha = -0.0207, \beta = 5.5060 \times 10^{-4}$ *(left column) and* $A = 14.6804, \alpha = 0, \beta = 0$ *(right column), corresponding to the* 0^{th} *and* 2^{nd} *order approximations, respectively. The degree of nonlocality is* $\omega_0/\mu = 3$*. Figs. a) and b) show the propagation along* Z/L_D *for* $Y/W_0 = 0$*, c) and d) show the variation of normalized intensity and width, and e) and f) show the transverse profile at i) the input, ii) the minimum value of intensity, iii) the maximum value of intensity and iv) the output.*

Figs. 4.5, 4.6 and 4.7 show propagation of these OAM beams in a Kerr medium with

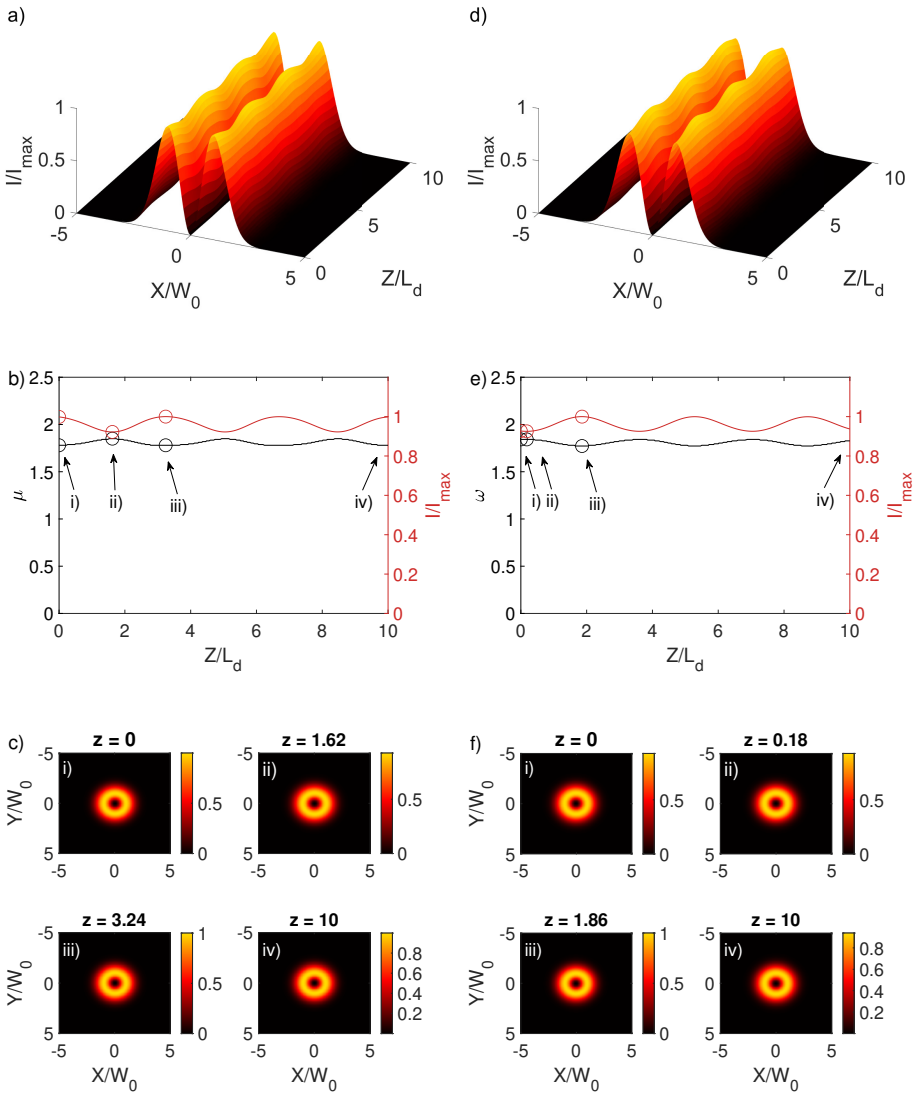

Figure 4.6. *Propagation of* ρ_{01} *with parameters* $A = 47.8874, \alpha = -0.0065, \beta = 5.6792 \times 10^{-5}$ *(left column) and* $A = 47.8874, \alpha = 0, \beta = 0$ *(right column), corresponding to the* 0^{th} *and* 2^{nd} *order approximations, respectively. The degree of nonlocality is* $\omega_0/\mu = 6$*. Figs. a) and b) show the propagation along* Z/L_D *for* $Y/W_0 = 0$*, c) and d) show the variation of normalized intensity and width, and e) and f) show the transverse profile at i) the input, ii) the minimum value of intensity, iii) the maximum value of intensity and iv) the output.*

different degrees of nonlocality. Once again, $\mu = 1$ across all figures. The initial width of each OAM beam is approximately $\sqrt{3}\mu$.

Fig. 4.5 shows the propagation of the an OAM beam where the degree of nonlocality is $\omega_0/(\sqrt{3}\mu) = 3/\sqrt{3} \approx 1.732$, which places in the case of general nonlocality. The variation in intensity is equal to 22.3745% for the 0^{th} order and 15.0516 for the 2^{nd} order, while the variations in width are 11.8162% and 6.7864% respectively.

Similarly, Fig. 4.6 shows the OAM beam in a degree of nonlocality $\omega_0/(\sqrt{3}\mu) = 6/\sqrt{3} \approx$

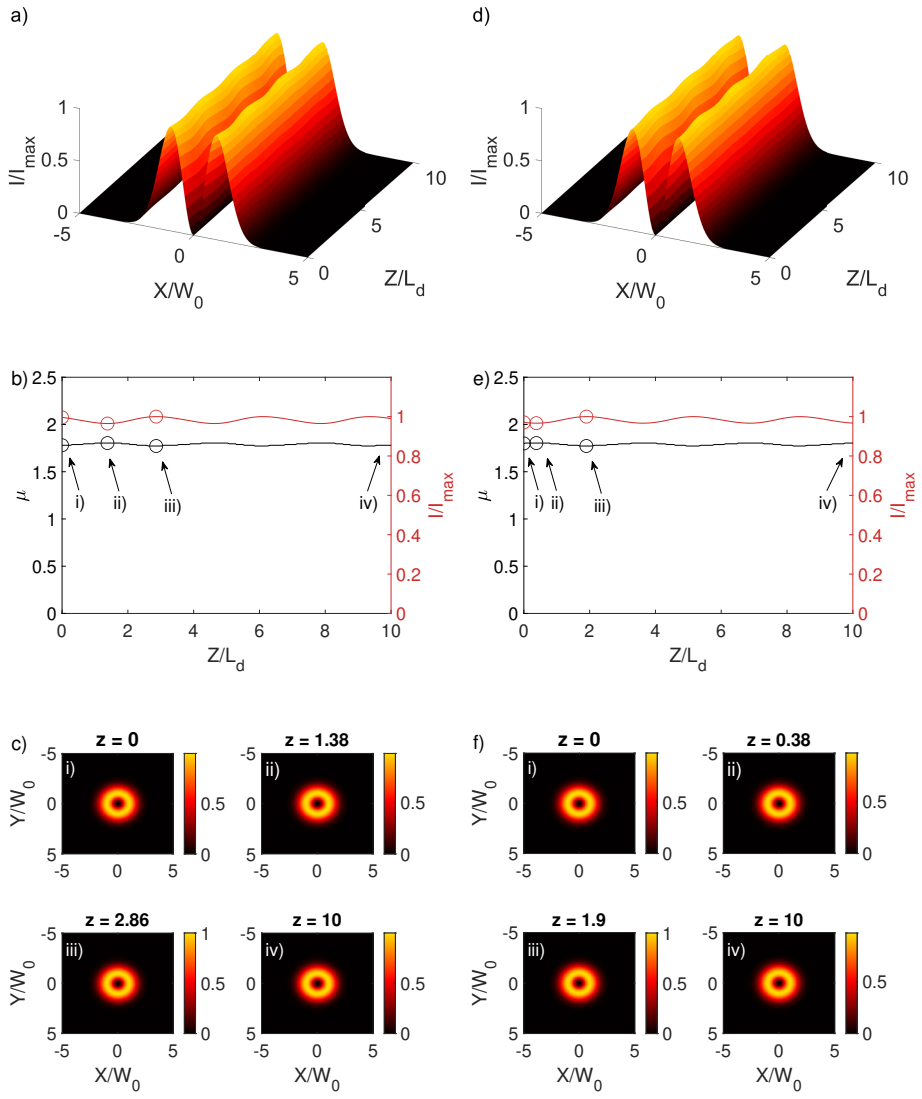

Figure 4.7. *Propagation of* ρ_{01} *with parameters* $A = 127.9390, \alpha = -0.0024, \beta = 7.9891 \times 10^{-6}$ *(left column) and* $A = 127.9390, \alpha = 0, \beta = 0$ *(right column), corresponding to the* 0^{th} *and* 2^{nd} *order approximations, respectively. The degree of nonlocality is* $\omega_0/\mu = 10$*. Figs. a) and b) show the propagation along* Z/L_D *for* $Y/W_0 = 0$*, c) and d) show the variation of normalized intensity and width, and e) and f) show the transverse profile at i) the input, ii) the minimum value of intensity, iii) the maximum value of intensity and iv) the output.*

3.464. The variation of intensity is 7.6508% for the 0^{th} order and 7.8819% for the 2^{nd} order. The width variations are 3.9387% and 3.8055% respectively.

Finally, Fig. 4.7 shows propagation of the OAM beam with degree of nonlocality $\omega_0/(\sqrt{3}\mu) = 10/\sqrt{3} \approx 5.77$, which places it within the case of general nonlocality. The variation in intensity is 3.132% for the 0^{th} order and 3.0086% for the 2^{nd} order, while the width varies 1.3129% and 1.5152% respectively.

Table 4.2. *Beam parameters of ρ_{01} for $\mu = 1$ and several values of ω_0. The width of the OAM carrying beam is $\sqrt{3}\mu$. Cases $\omega_0 = 3$, $\omega_0 = 6$ and $\omega_0 = 10$ all correspond to the generally nonlocal regime.*

	$\omega_0 = 3$	$\omega_0 = 6$	$\omega_0 = 10$
A	14.6804	47.8874	127.9390
α	-0.0207	-0.0065	-0.0024
β	5.5060×10^{-4}	5.6792×10^{-5}	7.9891×10^{-6}

Propagation of a vortex ring soliton such as ρ_{01} has been reported to decay into two fundamental solitons by sources such as [1, 5]. However, it is not observed in these simulations.

4.2 Propagation in media with exponential-decay nonlocality

The normalized nonlocal response function used to model an exponential-decay nonlocality is:

$$R(r) = \frac{1}{2\pi\omega_0^2} e^{-\frac{|r|}{\omega_0}}. \tag{4.2}$$

where ω_0 is the width of the function and it is normalized such that $\int_0^{2\pi}\int_0^{\infty} R(r) r dr d\theta = 1$. Fig. 4.8 shows the shape of the exponential-decay function. The procedure to obtain values for coefficients A, α and β is different in this case compared to the Gaussian nonlocality because the function is not twice differentiable at the origin. Instead, Eq. (3.3) is approximated analytically.

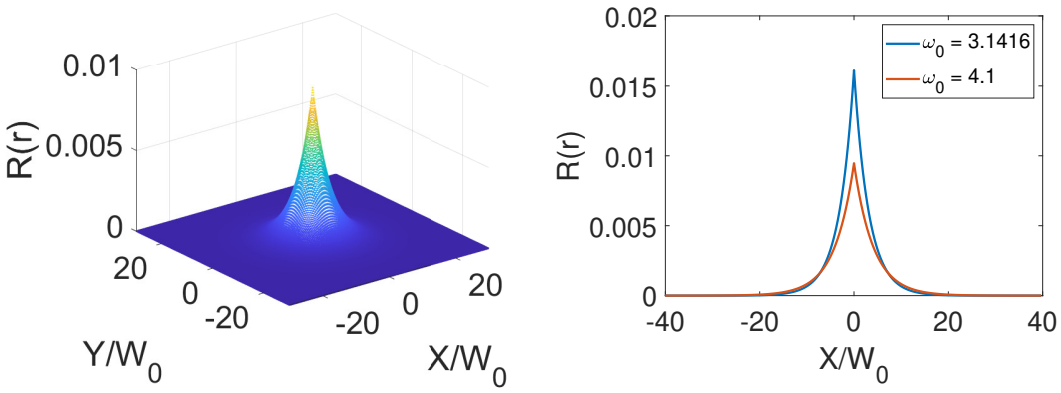

Figure 4.8. *Representation of an exponential-decay nonlocal response function. The figure shows a) the 3D profile for* $\omega_0 = 3.1416$ *and b) a 2D profile along* $Y/W_0 = 0$ *for different values of* ω_0*. The constraint imposed by the normalization condition has an effect on the magnitude of* $R(r)$*.*

To obtain the coefficients for Eq. (3.13), the approximation $\rho_{00} \approx \rho_{00}^{(0)}$ is taken, so that

$$\begin{aligned} V(r) &\approx -\int_0^{2\pi}\int_0^{\infty} \frac{1}{2\pi\omega_0^2} e^{-\frac{|\xi - r|}{\omega_0}} \frac{|A|^2}{\pi\mu^2} e^{-\frac{\xi^2}{\mu^2}} \xi d\xi d\theta \\ &= -\frac{|A|^2}{\pi\omega_0^2} e^{-\frac{r}{\omega_0}} e^{\frac{\mu^2}{4\omega_0^2}} \left[\frac{\sqrt{\pi}\mu}{4\omega_0} + \frac{1}{2}\right]. \end{aligned} \tag{4.3}$$

With this expression for $V(r)$, the coefficients can be approximated in terms of μ and ω_0 using Eqs. (3.8). The results are shown in the left column of 4.3 for $\mu = 1$ and $\omega_0 = 3.1416$. The degree of nonlocality is $\omega_0/\mu = 3.1416$, placing this example within the generally nonlocal case.

Similarly, Eq. (3.3) is approximated for the OAM case using $\rho_{01} \approx \rho_{01}^{(0)}$, which results in:

$$\begin{aligned} V(r) &\approx -\int_0^{2\pi}\int_0^{\infty} \frac{1}{2\pi\omega_0^2} e^{-\frac{|\xi - r|}{\omega_0}} \frac{|A|^2}{\pi\mu^2} e^{-\frac{\xi^2}{\mu^2}} \sqrt{\frac{\xi^2}{\mu^2}} \xi d\xi d\theta \\ &= -\frac{|A|^2}{\pi\omega_0^2} e^{-\frac{r}{\omega_0}} e^{\frac{\mu^2}{4\omega_0^2}} \left[\frac{\sqrt{\pi}}{4} + \frac{\mu}{2\omega_0} + \frac{\sqrt{\pi}\mu^2}{8\omega_0^2}\right]. \end{aligned} \tag{4.4}$$

This result is used with Eqs. (3.8) to obtain the value of the coefficients. These are listed in the right column of 4.3 for $\mu = 1$ and $\omega_0 = 4.1$. With the degree of nonlocality being $\omega_0/\sqrt{3}\mu = 2.367$, this case is also within the generally nonlocal regime.

Table 4.3. *Coefficients for the exponential-decay nonlocality. The values on the left column are used for the Non OAM-carrying beam, while the values on the right column are used for the OAM-carrying beam.*

	$\omega_0 = 3.1416$	$\omega_0 = 4.1$
A	21.5739	38.8917
α	-0.0042	-0.0029
β	-1.4258×10^{-5}	-6.0316×10^{-6}

4.2.1 Non OAM-carrying beam

Fig. 4.9 shows the propagation of the non OAM-carrying beam ρ_{00} in a medium with exponential nonlocality, with both the 0^{th} and 2^{nd} order approximations being shown. The maximum variation of the intensity is 9.3991% for the 0^{th} order and 9.1024% for the 2^{nd} order, with the variations in width being respectively 5.4475% and 6.1303%.

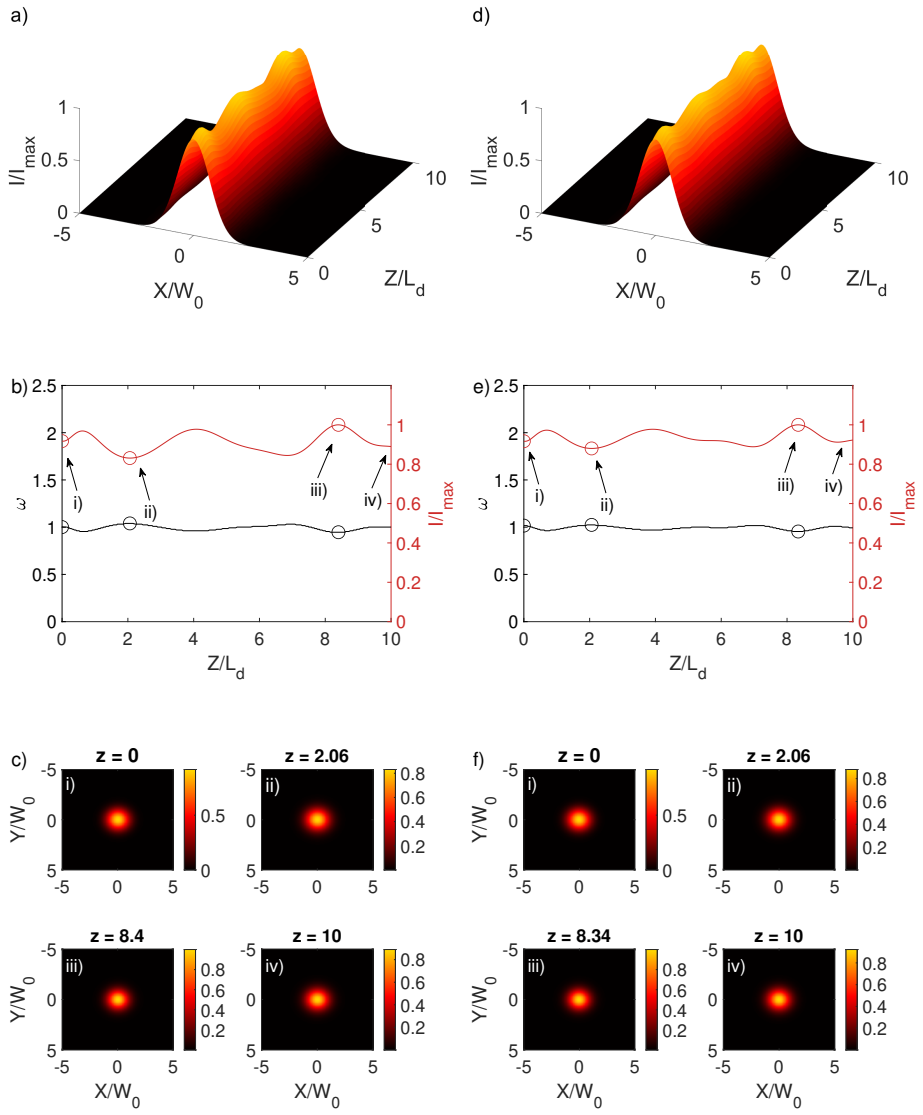

Figure 4.9. *Propagation of ρ_{00} in an exponential-decay type of nonlocality, with parameters $A = 21.5739, \alpha = -0.0042, \beta = -1.4258 \times 10^{-5}$ (left column) and $A = 21.5739, \alpha = 0, \beta = 0$ (right column), corresponding to the 0^{th} and 2^{nd} order approximations, respectively. The degree of nonlocality is $\omega_0/\mu = 3.1416$. Figs. a) and b) show the propagation along Z/L_D for $Y/W_0 = 0$, c) and d) show the variation of normalized intensity and width, and e) and f) show the transverse profile at i) the input, ii) the minimum value of intensity, iii) the maximum value of intensity and iv) the output. I_max is equal to 161.5164 for the 0^{th} order and 157.5105 for the 2^{nd} order.*

4.2.2 OAM-carrying beam

Fig. 4.10 displays the propagation of the OAM-carrying beam ρ_{01} is a medium with exponential-decay nonlocality. Both the 0^{th} and 2^{nd} orders are shown. The maximum variation in intensity is equal to 10.9488% for the 0^{th} order and 4.649% for the 2^{nd} order, while the maximum variations in width are 5.2516% and 2.1598% respectively.

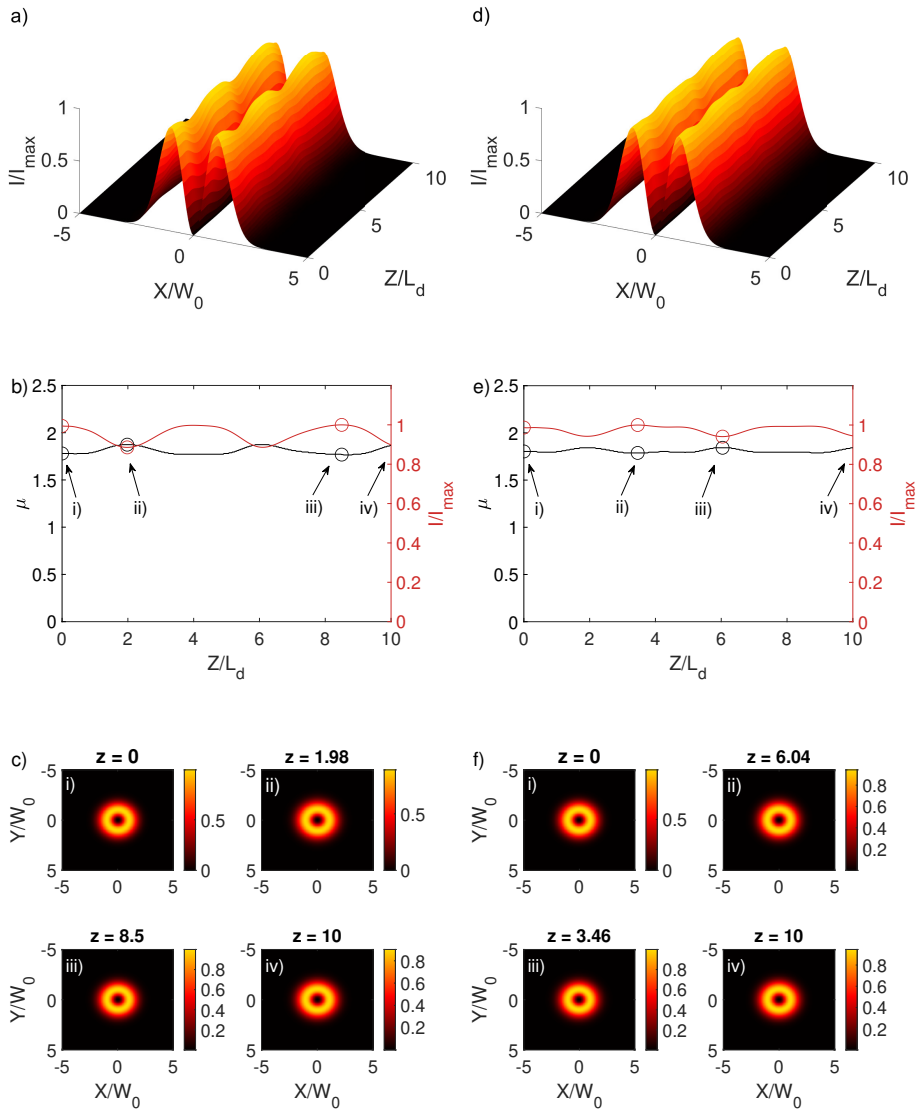

Figure 4.10. *Propagation of ρ_{01} in an exponential-decay type of nonlocality, with parameters $A = 38.8917, \alpha = -0.0029, \beta = -6.0316 \times 10^{-6}$ (left column) and $A = 38.8917, \alpha = 0, \beta = 0$ (right column), corresponding to the 0^{th} and 2^{nd} order approximations, respectively. The degree of nonlocality is $\omega_0/(\sqrt{3}\mu) = 2.367$. Figs. a) and b) show the propagation along Z/L_D for $Y/W_0 = 0$, c) and d) show the variation of normalized intensity and width, and e) and f) show the transverse profile at i) the input, ii) the minimum value of intensity, iii) the maximum value of intensity and iv) the output. I_max is equal to 178.1519 for the 0^{th} order and 173.7281 for the 2^{nd} order.*

Fig. 4.10 also shows one of the most significant improvements in the 2^{nd} order approximation when compared to the 0^{th} one. The following section discusses the most significant results in details, as well as making some remarking conclusions.

5. DISCUSSION AND CONCLUSIONS

This work has mainly focused on testing the stability of possible (2+1)D solitons in generally nonlocal media. The results have shown that the perturbation method produces profiles that are very close to a soliton state.

One of the most important outcomes of this work is providing evidence that the 2^{nd} order perturbative approximation improves significantly the description of the soliton state when compared to the 0^{th} order approximation, as can be observed in all Figures that show beam propagation (Figs. 4.2 to 4.4, 4.5 to 4.7 and 4.9 to 4.10).

The simulation shown in Fig. 4.3 indicates that the non OAM-carrying beam ρ_{00} describes the soliton in the generally nonlocal case to a very good degree. Similarly, Fig. 4.6 shows the OAM-carrying beam propagating close to the soliton state, which is significant proof that the perturbation method supports vortex solitons as well.

Particularly, beam ρ_{01} in the generally nonlocal regime of an exponential-decay type of nonlocaliy, as shown in Fig. 4.10, is scarcely explored in the literature. Skupin et al. [5] show a similar vortex soliton but the profile is described only in the strongly nonlocal case.

The author believes that working in the generally nonlocal case could provide several advantages over the strongly nonlocal regime due to its characteristic of generally requiring lower beam intensity. On a computational level, the generally nonlocal regime requires a smaller window size than the strongly nonlocal case, provided the soliton width μ remains the same. Tuning of the degree of nonlocality in nematic liquid crystals, which posses exponential-decay nonlocality, has been addressed in [40].

Future work regarding this topic would deal primarily with developing a complete family of perturbed LG modes. Even though the modes that are present on this thesis are the most significant, exploration of higher order LG modes is expected to be equally favorable. In fact, it is possible that more other radially symmetric beams could be described in terms of a family of these modes. Another significant work for the future is analyzing the optical phase of the OAM carrying beams, focusing on the effects of the nonlocality on this phase.

REFERENCES

[1] Kivshar, Y. S. and Agrawal, G. P. *Optical solitons: from fibers to photonic crystals*. Amsterdam ; Boston: Academic Press, 2003. ISBN: 978-0-12-410590-4.

[2] Agrawal, G. P. *Nonlinear fiber optics*. 4th ed. Quantum electronics–principles and applications. Amsterdam ; Boston: Elsevier / Academic Press, 2007. ISBN: 978-0-12-369516-1.

[3] Snyder, A. W. Accessible Solitons. en. *Science* 276.5318 (June 1997), pp. 1538–1541. ISSN: 00368075, 10959203. DOI: 10.1126/science.276.5318.1538. URL: https://www.sciencemag.org/lookup/doi/10.1126/science.276.5318.1538 (visited on 08/26/2021).

[4] Mollenauer, L. F. and Gordon, J. P. *Solitons in optical fibers: fundamentals and applications*. OCLC: ocm62290481. Amsterdam ; Boston: Elsevier/Academic Press, 2006. ISBN: 978-0-12-504190-4.

[5] Skupin, S., Bang, O., Edmundson, D. and Krolikowski, W. Stability of two-dimensional spatial solitons in nonlocal nonlinear media. en. *Physical Review E* 73.6 (June 2006), p. 066603. ISSN: 1539-3755, 1550-2376. DOI: 10.1103/PhysRevE.73.066603. URL: https://link.aps.org/doi/10.1103/PhysRevE.73.066603 (visited on 08/20/2021).

[6] Suter, D. and Blasberg, T. Stabilization of transverse solitary waves by a nonlocal response of the nonlinear medium. en. *Physical Review A* 48.6 (Dec. 1993), pp. 4583–4587. ISSN: 1050-2947, 1094-1622. DOI: 10.1103/PhysRevA.48.4583. URL: https://link.aps.org/doi/10.1103/PhysRevA.48.4583 (visited on 10/18/2021).

[7] Conti, C., Peccianti, M. and Assanto, G. Observation of Optical Spatial Solitons in a Highly Nonlocal Medium. en. *Physical Review Letters* 92.11 (Mar. 2004), p. 113902. ISSN: 0031-9007, 1079-7114. DOI: 10.1103/PhysRevLett.92.113902. URL: https://link.aps.org/doi/10.1103/PhysRevLett.92.113902 (visited on 10/06/2021).

[8] Drazin, P. G. and Johnson, R. S. *Solitons: an introduction*. Cambridge texts in applied mathematics 2. Cambridge [England] ; New York: Cambridge University Press, 1989. ISBN: 978-0-521-33389-4 978-0-521-33655-0.

[9] S. Trillo, W. Torruellas and W. T. Rhodes, eds. *Spatial Solitons*. en. Vol. 82. Springer Series in Optical Sciences. Berlin, Heidelberg: Springer Berlin Heidelberg, 2001. ISBN: 978-3-642-07498-1 978-3-540-44582-1. DOI: 10.1007/978-3-540-44582-

1. URL: http://link.springer.com/10.1007/978-3-540-44582-1 (visited on 10/06/2021).

[10] Conti, C., Peccianti, M. and Assanto, G. Route to Nonlocality and Observation of Accessible Solitons. en. *Physical Review Letters* 91.7 (Aug. 2003), p. 073901. ISSN: 0031-9007, 1079-7114. DOI: 10.1103/PhysRevLett.91.073901. URL: https://link.aps.org/doi/10.1103/PhysRevLett.91.073901 (visited on 10/06/2021).

[11] Ablowitz, J. Analytical and Numerical Aspects of Certain Nonlinear Evolution Equations. II. Numerical, Nonlinear Schradinger Equation. en. (), p. 28.

[12] Bang, O., Krolikowski, W., Wyller, J. and Rasmussen, J. J. Collapse arrest and soliton stabilization in nonlocal nonlinear media. en. *Physical Review E* 66.4 (Oct. 2002), p. 046619. ISSN: 1063-651X, 1095-3787. DOI: 10.1103/PhysRevE.66.046619. URL: https://link.aps.org/doi/10.1103/PhysRevE.66.046619 (visited on 09/09/2021).

[13] Malomed, B. A. Fundamental nonlinear equations in physics and their fundamental solutions. en. (), p. 61.

[14] Deng, D., Guo, Q. and Hu, W. Hermite Laguerre Gaussian beams in strongly nonlocal nonlinear media. en. (2008), p. 5.

[15] Guo, Q., Luo, B., Yi, F., Chi, S. and Xie, Y. Large phase shift of nonlocal optical spatial solitons. en. *Physical Review E* 69.1 (Jan. 2004), p. 016602. ISSN: 1539-3755, 1550-2376. DOI: 10.1103/PhysRevE.69.016602. URL: https://link.aps.org/doi/10.1103/PhysRevE.69.016602 (visited on 08/28/2021).

[16] Krolikowski, W., Bang, O., Rasmussen, J. J. and Wyller, J. Modulational instability in nonlocal nonlinear Kerr media. en. *Physical Review E* 64.1 (June 2001), p. 016612. ISSN: 1063-651X, 1095-3787. DOI: 10.1103/PhysRevE.64.016612. URL: https://link.aps.org/doi/10.1103/PhysRevE.64.016612 (visited on 09/09/2021).

[17] Baizakov, B. B., Malomed, B. A. and Salerno, M. Multidimensional solitons in periodic potentials. en. *Europhysics Letters (EPL)* 63.5 (Sept. 2003), pp. 642–648. ISSN: 0295-5075, 1286-4854. DOI: 10.1209/epl/i2003-00579-4. URL: https://iopscience.iop.org/article/10.1209/epl/i2003-00579-4 (visited on 08/28/2021).

[18] Malomed, B. A. Multidimensional solitons: Well-established results and novel findings. en. *The European Physical Journal Special Topics* 225.13-14 (Nov. 2016), pp. 2507–2532. ISSN: 1951-6355, 1951-6401. DOI: 10.1140/epjst/e2016-60025-y. URL: http://link.springer.com/10.1140/epjst/e2016-60025-y (visited on 08/20/2021).

[19] Huang, Y., Guo, Q. and Cao, J. Optical beams in lossy non-local Kerr media. en. *Optics Communications* 261.1 (May 2006), pp. 175–180. ISSN: 00304018. DOI: 10.1016/j.optcom.2005.12.003. URL: https://linkinghub.elsevier.com/retrieve/pii/S003040180501312X (visited on 08/29/2021).

[20] Guo, Q., Luo, B. and Chi, S. Optical beams in sub-strongly non-local nonlinear media: A variational solution. en. *Optics Communications* 259.1 (Mar. 2006), pp. 336–341. ISSN: 00304018. DOI: 10.1016/j.optcom.2005.08.067. URL: https://linkinghub.elsevier.com/retrieve/pii/S0030401805009120 (visited on 09/17/2021).

[21] Ouyang, S., Guo, Q. and Hu, W. Perturbative analysis of generally nonlocal spatial optical solitons. en. *Physical Review E* 74.3 (Sept. 2006). arXiv: physics/0609163, p. 036622. ISSN: 1539-3755, 1550-2376. DOI: 10.1103/PhysRevE.74.036622. URL: http://arxiv.org/abs/physics/0609163 (visited on 08/20/2021).

[22] Deng, D. and Guo, Q. Propagation of Laguerre–Gaussian beams in nonlocal nonlinear media. en. *Journal of Optics A: Pure and Applied Optics* 10.3 (Mar. 2008), p. 035101. ISSN: 1464-4258, 1741-3567. DOI: 10.1088/1464-4258/10/3/035101. URL: https://iopscience.iop.org/article/10.1088/1464-4258/10/3/035101 (visited on 09/16/2021).

[23] Nikolov, N. I., Neshev, D., Bang, O. and Królikowski, W. Z. Quadratic solitons as nonlocal solitons. en. *Physical Review E* 68.3 (Sept. 2003), p. 036614. ISSN: 1063-651X, 1095-3787. DOI: 10.1103/PhysRevE.68.036614. URL: https://link.aps.org/doi/10.1103/PhysRevE.68.036614 (visited on 08/20/2021).

[24] Kelley, P. L. Self-Focusing of Optical Beams. en. *Physical Review Letters* 15.26 (Dec. 1965), pp. 1005–1008. ISSN: 0031-9007. DOI: 10.1103/PhysRevLett.15.1005. URL: https://link.aps.org/doi/10.1103/PhysRevLett.15.1005 (visited on 08/20/2021).

[25] Doktorov, E. V. and Molchan, M. A. Soliton train dynamics in a weakly nonlocal non-Kerr nonlinear medium. en. *Journal of Physics A: Mathematical and Theoretical* 41.31 (Aug. 2008), p. 315101. ISSN: 1751-8113, 1751-8121. DOI: 10.1088/1751-8113/41/31/315101. URL: https://iopscience.iop.org/article/10.1088/1751-8113/41/31/315101 (visited on 08/20/2021).

[26] Królikowski, W. and Bang, O. Solitons in nonlocal nonlinear media: Exact solutions. en. *Physical Review E* 63.1 (Dec. 2000), p. 016610. ISSN: 1063-651X, 1095-3787. DOI: 10.1103/PhysRevE.63.016610. URL: https://link.aps.org/doi/10.1103/PhysRevE.63.016610 (visited on 08/20/2021).

[27] Trejo-Garcia, D., Gonzalez-Hernandez, D., López-Aguayo, D. and Lopez-Aguayo, S. Stable Hermite-Gaussian solitons in optical lattices. en. *Journal of Optics* 20.12 (Dec. 2018), p. 125501. ISSN: 2040-8978, 2040-8986. DOI: 10.1088/2040-8986/aaea46. URL: https://iopscience.iop.org/article/10.1088/2040-8986/aaea46 (visited on 10/18/2021).

[28] Chiao, R. Y., Garmire, E. and Townes, C. H. Self-Trapping of Optical Beams. en. *Physical Review Letters* 13.15 (Oct. 1964), pp. 479–482. ISSN: 0031-9007. DOI: 10.1103/PhysRevLett.13.479. URL: https://link.aps.org/doi/10.1103/PhysRevLett.13.479 (visited on 10/21/2021).

[29] Boyd, R. W. *Nonlinear optics*. 2nd ed. San Diego, CA: Academic Press, 2003. ISBN: 978-0-12-121682-5.

[30] Griffiths, D. J. *Introduction to electrodynamics*. 3rd ed. Upper Saddle River, N.J: Prentice Hall, 1999. ISBN: 978-0-13-805326-0.

[31] Nikolov, N. I., Neshev, D., Królikowski, W., Bang, O., Rasmussen, J. J. and Christiansen, P. L. Attraction of nonlocal dark optical solitons. en. *Optics Letters* 29.3 (Feb. 2004), p. 286. ISSN: 0146-9592, 1539-4794. DOI: 10.1364/OL.29.000286. URL: https://www.osapublishing.org/abstract.cfm?URI=ol-29-3-286 (visited on 08/24/2021).

[32] Królikowski, W., Bang, O. and Wyller, J. Nonlocal incoherent solitons. en. *Physical Review E* 70.3 (Sept. 2004), p. 036617. ISSN: 1539-3755, 1550-2376. DOI: 10.1103/PhysRevE.70.036617. URL: https://link.aps.org/doi/10.1103/PhysRevE.70.036617 (visited on 08/28/2021).

[33] Greiner, W. *Quantum mechanics: an introduction*. eng. 4th ed. Berlin ; New York: Springer, 2001. ISBN: 978-3-540-67458-0.

[34] Griffiths, D. J. *Introduction to quantum mechanics*. eng. 2. ed. Pearson international edition. Upper Saddle River, NJ London: Pearson Prentice Hall, 2005. ISBN: 978-0-13-191175-8 978-0-13-111892-8.

[35] Beijersbergen, M. W., Coerwinkel, R. P. C. and Kristensen, M. Helical-wavefront laser beams produced with a spiral phaseplate. en. (), p. 7.

[36] Shen, Y., Wang, X., Xie, Z., Min, C., Fu, X., Liu, Q., Gong, M. and Yuan, X. Optical vortices 30 years on: OAM manipulation from topological charge to multiple singularities. en. *Light: Science & Applications* 8.1 (Dec. 2019), p. 90. ISSN: 2047-7538. DOI: 10.1038/s41377-019-0194-2. URL: http://www.nature.com/articles/s41377-019-0194-2 (visited on 10/26/2021).

[37] Byron, F. W. and Fuller, R. W. *Mathematics of classical and quantum physics*. New York: Dover Publications, 1992. ISBN: 978-0-486-67164-2.

[38] Messiah, A. *Quantum Mechanics.* English. OCLC: 874097814. Dover Publications, 2014. ISBN: 978-1-306-51279-4 978-0-486-79166-1 978-0-486-78455-7. URL: http://www.myilibrary.com?id=582530 (visited on 10/23/2021).

[39] Arfken, G. *Mathematical methods for physicists*. eng. 3. ed., 7. [print.] San Diego, Calif.: Academic Pr, 1993. ISBN: 978-0-12-059810-6 978-0-12-059820-5.

[40] Peccianti, M., Conti, C. and Assanto, G. Interplay between nonlocality and nonlinearity in nematic liquid crystals. en. *Optics Letters* 30.4 (Feb. 2005), p. 415. ISSN: 0146-9592, 1539-4794. DOI: 10.1364/OL.30.000415. URL: https://www.osapublishing.org/abstract.cfm?URI=ol-30-4-415 (visited on 10/27/2021).

[41] Gradshteĭn, I. S., Ryzhik, I. M. and Jeffrey, A. *Table of integrals, series, and products*. en. 7th ed. Amsterdam ; Boston: Academic Press, 2007. ISBN: 978-0-12-373637-6.

[42] Dirac, P. A. M. *The principles of quantum mechanics*. eng. New York: Snowball Publishing, 2013. ISBN: 978-1-60796-560-2.

APPENDIX A: HARMONIC OSCILLATOR IN CYLINDRICAL COORDINATES

This appendix shows how to solve of Eq. (3.9) with $\alpha = \beta = 0$, which corresponds to the unperturbed case

$$\left[-\frac{1}{2}\frac{d^2}{dr^2} - \frac{1}{2r}\frac{d}{dr} + \frac{m^2}{2r^2} + \frac{1}{2\mu^4}r^2\right]\rho = \varepsilon\rho, \tag{A.1}$$

where $\rho = \rho(r)$ is the radial part of Eq. (3.2). A change of variable of the form

$$x = \frac{r^2}{\mu^2} \tag{A.2}$$

allows to rewrite Eq. A.1 in the following way:

$$\frac{d^2\rho}{dx^2} + \frac{1}{x}\frac{d\rho}{dx} + \left(\frac{\varepsilon\mu^2}{2x} - \frac{m^2}{4x^2} - \frac{1}{4}\right)\rho = 0. \tag{A.3}$$

This equation has an Ansatz that will provide Laguerre-Gaussian solutions

$$\rho = x^{\frac{|m|}{2}} e^{-\frac{x}{2}}\chi(x) \tag{A.4}$$

Substitution of Ansatz A.4 in Eq. A.3 leads to a differential equation for $\chi(x)$. This is the equation for the generalized Laguerre polynomials.

$$x\frac{d^2\chi}{dx^2} + (m+1-x)\frac{d\chi}{dx} + \left(\frac{\varepsilon\mu^2}{2} - \frac{m}{2} - \frac{1}{2}\right)\chi = 0. \tag{A.5}$$

Solutions to (A.5) have the form:

$$\rho^{(0)}_{km}(r) = A_\rho \left(\frac{r^2}{\mu^2}\right)^{\frac{|m|}{2}} e^{-\frac{r^2}{2\mu^2}} L_{km}\left(\frac{r^2}{\mu^2}\right) \tag{A.6}$$

Where A_ρ is a normalization constant. Normalization requires that

$$1 = A_\rho^2 \int_0^\infty \int_0^{2\pi} |u(r,\theta,z)|^2 r dr, \tag{A.7}$$

where A_ρ is the radial normalization constant. Substituting (3.2) and (3.5) in the last equation leads to

$$A_\rho^2 \int_0^\infty |\rho(r)|^2 r dr = 1. \tag{A.8}$$

After a change of variable as in Eq. (A.2):

$$A_\rho^2 \frac{\mu^2}{2} \int_0^\infty x^{|m|} e^{-x} \left[L_k^m(x)\right]^2 dx = 1, \tag{A.9}$$

the integral in Eq. (A.9) can be solved using the orthogonality properties of generalized Laguerre polynomials, as indicated in Eq. 3 of section 7.414 of [41]. The result is

$$A_\rho = \sqrt{\frac{2k!}{\mu^2 \Gamma(m+k+1)}}. \tag{A.10}$$

This yields the normalized solution to the unperturbed problem:

$$u_{km}^{(0)}(r,\theta,z) = \frac{1}{\sqrt{2\pi}} \sqrt{\frac{2k!}{\mu^2 \Gamma(m+k+1)}} \left(\frac{r^2}{\mu^2}\right)^{\frac{|m|}{2}} e^{-\frac{r^2}{2\mu^2}} L_{km}\left(\frac{r^2}{\mu^2}\right) e^{i\theta m} e^{-i(\varepsilon+V_0)z}. \tag{A.11}$$

APPENDIX B: PERTURBED FUNDAMENTAL SOLUTION

Eq. (3.9) resembles a Schrödinger equation, with a perturbation

$$H' = \alpha r^4 + \beta r^6. \tag{B.1}$$

Using perturbation theory up to the second order correction will yiled a solution of the following shape (from this point on, the r dependency is omitted for simplicity):

$$\rho_{km} = \rho_{km}^{(0)} + \lambda \rho_{km}^{(1)} + \lambda^2 \rho_{km}^{(2)}. \tag{B.2}$$

0^{th} approximation to the fundamental case

The first term of the RHS of (B.2) corresponds to the unperturbed case in Eq. (A.6) and was calculated in Appendix A, with values of $k = m = 0$

$$\rho_{00}^{(0)} = \frac{\sqrt{2}}{\mu} e^{-\frac{r^2}{2\mu^2}}. \tag{B.3}$$

1^{st} order approximation to the fundamental case

Generally, the first order approximation for a given state ρ_{pn} in the nondegenerate case, requires us to solve

$$|\rho_{pn}^{(1)}\rangle = \sum_{k \neq p} \sum_{m \neq n} \frac{\langle \rho_{km}^{(0)} | H' | \rho_{pn}^{(0)} \rangle}{\varepsilon_{pn}^{(0)} - \varepsilon_{km}^{(0)}} \, |\rho_{km}^{(0)}\rangle \,, \tag{B.4}$$

where, for the sake of simplicity, Dirac's bra-ket notation [42] has been employed. Using the unperturbed state and energy expressions in (3.10) and (3.11) respectively, as well as the change of variable defined in (A.2), it can be written

$$|\rho_{pn}^{(1)}\rangle = \sum_{m\neq n}^{\infty}\sum_{k\neq p}^{\infty}\left(\frac{\mu^2}{2(p-k)+n-m}\right)\left(\frac{2k!}{\mu^2\Gamma(m+k+1)}\right)\sqrt{\frac{2p!}{\mu^2\Gamma(n+p+1)}} \times \int x^{\frac{m+n}{2}}e^{-x}L_k^m(x)L_p^n(x)\left[\alpha\mu^4x^2+\beta\mu^6x^3\right]dx\,|\rho_{km}^{(0)}\rangle \tag{B.5}$$

Now, for the case of $p=n=0$

$$|\rho_{00}^{(1)}\rangle = \sum_{m\neq 0}^{\infty}\sum_{k\neq 0}^{\infty}\left(-\frac{2\sqrt{2}k!}{\mu(2k+m)\Gamma(m+k+1)}\right) \times\left[\alpha\mu^4\int x^{\frac{m}{2}+2}e^{-x}L_k^m(x)dx+\beta\mu^6\int x^{\frac{m}{2}+3}e^{-x}L_k^m(x)dx\right]|\rho_{km}^{(0)}\rangle \tag{B.6}$$

The integrals in expression (B.6) may be solved analytically using equation 7 from section 7.414 of [41]. This gives:

$$|\rho_{00}^{(1)}\rangle = \sum_{m\neq 0}^{\infty}\sum_{k\neq 0}^{\infty}\left(-\frac{2\sqrt{2}}{\mu(2k+m)}\right)\left[\alpha\mu^4\frac{\Gamma(\frac{m}{2}+3)}{\Gamma(m+1)}\,{}_2F_1\left(-k,\frac{m}{2}+3;m+1;1\right) + \beta\mu^6\frac{\Gamma(\frac{m}{2}+4)}{\Gamma(m+1)}{}_2F_1\left(-k,\frac{m}{2}+4;m+1;1\right)\right]|\rho_{km}^{(0)}\rangle\,, \tag{B.7}$$

where ${}_2F_1$ is the hypergeometric function.

2nd order approximation to the fundamental case

The second order perturbation of any ρ_{pn} comes from the following equation containing three terms

$$\begin{aligned}|\rho_{pn}^{(2)}\rangle =& \sum_{k\neq p}\sum_{m\neq n}\sum_{q\neq p}\sum_{s\neq n}\frac{\langle\rho_{km}^{(0)}|H'|\rho_{qs}^{(0)}\rangle\,\langle\rho_{qs}^{(0)}|H'|\rho_{pn}^{(0)}\rangle}{(\varepsilon_{pn}^{(0)}-\varepsilon_{km}^{(0)})(\varepsilon_{pn}^{(0)}-\varepsilon_{qs}^{(0)})}\,|\rho_{km}^{(0)}\rangle \\ &-\sum_{k\neq p}\sum_{m\neq n}\frac{\langle\rho_{km}^{(0)}|H'|\rho_{pn}^{(0)}\rangle\,\langle\rho_{pn}^{n(0)}|H'|\rho_{pn}^{(0)}\rangle}{(\varepsilon_{pn}^{(0)}-\varepsilon_{km}^{(0)})^2}\,|\rho_{km}^{(0)}\rangle \\ &-\frac{1}{2}\,|\rho_{pn}^{(0)}\rangle\sum_{k\neq p}\sum_{m\neq n}\frac{|\,\langle\rho_{km}^{(0)}|H'|\rho_{pn}^{(0)}\rangle\,|^2}{(\varepsilon_{pn}^{(0)}-\varepsilon_{km}^{(0)})^2}.\end{aligned} \tag{B.8}$$

In this Appendix, each term is calculated separately, such that

$$|\rho_{pn}^{(2)}\rangle = |t_1\rangle - |t_2\rangle - |t_3\rangle\,. \tag{B.9}$$

First term:

$$\begin{aligned}|t_1\rangle =& \sum_{k\neq p}\sum_{m\neq n}\sum_{q\neq p}\sum_{s\neq n}\left(\frac{\mu^2}{2(p-k)+n-m}\right)\left(\frac{\mu^2}{2(p-q)+n-s}\right)\\ &\times\left(\frac{2k!}{\mu^2\Gamma(m+k+1)}\right)\left(\frac{2q!}{\mu^2\Gamma(s+q+1)}\right)\sqrt{\frac{2p!}{\mu^2\Gamma(n+p+1)}}\\ &\times\int x^{\frac{m+s}{2}}e^{-x}L_k^m(x)L_q^s(x)\left[\alpha\mu^4x^2+\beta\mu^6x^3\right]dx\\ &\times\int x^{\frac{q+s}{2}}e^{-x}L_q^s(x)L_p^n(x)\left[\alpha\mu^4x^2+\beta\mu^6x^3\right]dx\,|\rho_{km}^{(0)}\rangle\end{aligned} \tag{B.10}$$

Substitution of $p=n=0$ changes the equation accordingly:

$$\begin{aligned}|t_1\rangle =& \sum_{k\neq 0}\sum_{m\neq 0}\sum_{q\neq 0}\sum_{s\neq 0}\left(-\frac{\mu^2}{2k+m}\right)\left(-\frac{\mu^2}{2q+s}\right)\left(\frac{2k!}{\mu^2\Gamma(m+k+1)}\right)\\ &\times\left(\frac{2q!}{\mu^2\Gamma(s+q+1)}\right)\sqrt{\frac{2}{\mu^2}}\int x^{\frac{m+s}{2}}e^{-x}L_k^m(x)L_q^s(x)\left[\alpha\mu^4x^2+\beta\mu^6x^3\right]dx\\ &\times\int x^{\frac{s}{2}}e^{-x}L_q^s(x)\left[\alpha\mu^4x^2+\beta\mu^6x^3\right]dx\,|\rho_{km}^{(0)}\rangle\,.\end{aligned} \tag{B.11}$$

The method to solve the second integral in the previous equation has already been shown in Eq. (B.6). On the other hand, the first integral is labeled as I_{t_1}:

$$I_{t_1} = \int x^{\frac{m+s}{2}}e^{-x}L_k^m(x)L_q^s(x)\left[\alpha\mu^4x^2+\beta\mu^6x^3\right]dx \tag{B.12}$$

$$I_{t_1} = \alpha\mu^4\int x^{\frac{m+s}{2}+2}e^{-x}L_k^m(x)L_q^s(x)dx + \beta\mu^6\int x^{\frac{m+s}{2}+3}e^{-x}L_k^m(x)L_q^s(x)dx \tag{B.13}$$

Eq. (B.13) can be integrated by parts, taking $u = x^{2-\frac{m+h}{2}}$ and $dv = e^{-x}x^{m+h}L_k^m(x)L_g^h(x)dx$ for the first integral and likewise for the second one. Using Eq. 4(1) from Section 7.414 of [41], both integrals turn out to be zero, meaning

$$|t_1\rangle = 0. \tag{B.14}$$

Proceeding with t_2,

$$|t_2\rangle = \sum_{k\neq p}\sum_{m\neq n} \frac{\langle \rho_k^{m(0)}|H'|\rho_p^{n(0)}\rangle \langle \rho_p^{n(0)}|H'|\rho_p^{n(0)}\rangle}{(\varepsilon_p^{n(0)} - \varepsilon_k^{m(0)})^2} |\rho_{km}^{(0)}\rangle \,. \tag{B.15}$$

In the general case for any p and n.

$$\begin{aligned} |t_2\rangle = &\sum_{k\neq p}\sum_{m\neq n} \left(\frac{\mu^2}{2(p-k)+n-m}\right)^2 \left(\frac{2k!}{\mu^2\Gamma(m+k+1)}\right) \\ &\times \left(\frac{2p!}{\mu^2\Gamma(n+p+1)}\right)^{\frac{3}{2}} \int x^{\frac{m+n}{2}} e^{-x} L_k^m(x) L_p^n(x) \left[\alpha\mu^4 x^2 + \beta\mu^6 x^3\right] dx \\ &\times \int x^n e^{-x} \left[L_p^n(x)\right]^2 \left[\alpha\mu^4 x^2 + \beta\mu^6 x^3\right] dx \, |\rho_{km}^{(0)}\rangle \end{aligned} \tag{B.16}$$

Now, for the fundamental solution $p = n = 0$:

$$\begin{aligned} |t_2\rangle = &\sum_{k\neq 0}\sum_{m\neq 0} \left(-\frac{\mu^2}{2k+m}\right)^2 \left(\frac{2k!}{\mu^2\Gamma(m+k+1)}\right) \left(\frac{2}{\mu^2\Gamma(1)}\right)^{\frac{3}{2}} \\ &\times \int x^{\frac{m}{2}} e^{-x} L_k^m(x) \left[\alpha\mu^4 x^2 + \beta\mu^6 x^3\right] dx \\ &\times \int e^{-x} \left[\alpha\mu^4 x^2 + \beta\mu^6 x^3\right] dx \, |\rho_{km}^{(0)}\rangle \end{aligned} \tag{B.17}$$

$$\begin{aligned} |t_2\rangle = &\sum_{k\neq 0}\sum_{m\neq 0} \left(-\frac{\mu^2}{2k+m}\right)^2 \left(\frac{2k!}{\mu^2\Gamma(m+k+1)}\right) \left(\frac{2}{\mu^2\Gamma(1)}\right)^{\frac{3}{2}} \\ &\times \left[\alpha\mu^4 \int x^{\frac{m}{2}+2} e^{-x} L_k^m(x) dx + \beta\mu^6 \int x^{\frac{m}{2}+3} e^{-x} L_k^m(x) dx\right] \\ &\times \left[\alpha\mu^4 \int e^{-x} x^2 dx + \beta\mu^6 \int e^{-x} x^3 dx\right] |\rho_{km}^{(0)}\rangle \end{aligned} \tag{B.18}$$

$$
\begin{aligned}
|t_2\rangle =& \sum_{k\neq 0}\sum_{m\neq 0}\left(-\frac{\mu^2}{2k+m}\right)^2\left(\frac{2k!}{\mu^2\Gamma(m+k+1)}\right)\left(\frac{2}{\mu^2\Gamma(1)}\right)^{\frac{3}{2}} \\
&\times\left[\alpha\mu^4\int x^{\frac{m}{2}+2}e^{-x}L_k^m(x)dx+\beta\mu^6\int x^{\frac{m}{2}+3}e^{-x}L_k^m(x)dx\right] \\
&\times\left[2\alpha\mu^4+6\beta\mu^6\right]|\rho_{km}^{(0)}\rangle
\end{aligned}
\tag{B.19}
$$

Solving the previous expression is similar to Eqs. (C.3) and (**??**).

$$
\begin{aligned}
|t_2\rangle =& \sum_{k\neq 0}\sum_{m\neq 0}\left(-\frac{\mu^2}{2k+m}\right)^2\left(\frac{2k!}{\mu^2\Gamma(m+k+1)}\right)\left(\frac{2}{\mu^2\Gamma(1)}\right)^{\frac{3}{2}} \\
&\times\left[\alpha\mu^4\frac{\Gamma(\frac{m}{2}+3)\Gamma(m+k+1)}{k!\Gamma(m+1)}{}_2F_1\left(-k,\frac{m}{2}+3;m+1;1\right)\right. \\
&\left.+\beta\mu^6\frac{\Gamma(\frac{m}{2}+4)\Gamma(m+k+1)}{k!\Gamma(m+1)}{}_2F_1\left(-k,\frac{m}{2}+4;m+1;1\right)\right] \\
&\times\left[2\alpha\mu^4+6\beta\mu^6\right]|\rho_{km}^{(0)}\rangle
\end{aligned}
\tag{B.20}
$$

$$
\begin{aligned}
|t_2\rangle =& \sum_{k\neq 0}\sum_{m\neq 0}\left(-\frac{\mu^2}{2k+m}\right)^2\left(\frac{2}{\mu^2}\right)\left(\frac{2^{\frac{3}{2}}}{\mu^3}\right) \\
&\times\left[\alpha\mu^4\frac{\Gamma(\frac{m}{2}+3)}{\Gamma(m+1)}{}_2F_1\left(-k,\frac{m}{2}+3;m+1;1\right)\right. \\
&\left.+\beta\mu^6\frac{\Gamma(\frac{m}{2}+4)}{\Gamma(m+1)}{}_2F_1\left(-k,\frac{m}{2}+4;m+1;1\right)\right] \\
&\times\left[2\alpha\mu^4+6\beta\mu^6\right]|\rho_{km}^{(0)}\rangle
\end{aligned}
\tag{B.21}
$$

Regarding the last term:

$$
|t_3\rangle = \frac{1}{2}|\rho_p^{n(0)}\rangle\sum_{k\neq p}\sum_{m\neq n}\frac{|\langle\rho_k^{m(0)}|H'|\rho_p^{n(0)}\rangle|^2}{(\varepsilon_p^{n(0)}-\varepsilon_k^{m(0)})^2}
\tag{B.22}
$$

$$
\begin{aligned}
|t_3\rangle =& \frac{1}{2}\sum_{m\neq n}^{\infty}\sum_{k\neq p}^{\infty}\left(\frac{\mu^2}{2(p-k)+n-m}\right)^2\left(\frac{2k!}{\mu^2\Gamma(m+k+1)}\right)\left(\frac{2p!}{\mu^2\Gamma(n+p+1)}\right)^{\frac{3}{2}} \\
&\times\left|\int x^{\frac{m+n}{2}}e^{-x}L_k^m(x)L_p^n(x)\left[\alpha\mu^4x^2+\beta\mu^6x^3\right]dx\right|^2|\rho_{pn}^{(0)}\rangle
\end{aligned}
\tag{B.23}
$$

Fundamental case $p = n = 0$:

$$|t_3\rangle = \frac{1}{2}\sum_{m\neq 0}^{\infty}\sum_{k\neq 0}^{\infty}\left(-\frac{\mu^2}{2k+m}\right)^2\left(\frac{2k!}{\mu^2\Gamma(m+k+1)}\right)\left(\frac{2}{\mu^2\Gamma(1)}\right)^{\frac{3}{2}} \times\left|\int x^{\frac{m}{2}}e^{-x}L_k^m(x)\left[\alpha\mu^4x^2+\beta\mu^6x^3\right]dx\right|^2|\rho_{pn}^{(0)}\rangle \tag{B.24}$$

$$|t_3\rangle = \frac{1}{2}\sum_{m\neq 0}^{\infty}\sum_{k\neq 0}^{\infty}\left(-\frac{\mu^2}{2k+m}\right)^2\left(\frac{2k!}{\mu^2\Gamma(m+k+1)}\right)\left(\frac{2}{\mu^2\Gamma(1)}\right)^{\frac{3}{2}} \times\left|\alpha\mu^4\int x^{\frac{m}{2}+2}e^{-x}L_k^m(x)dx+\beta\mu^6\int x^{\frac{m}{2}+3}e^{-x}L_k^m(x)dx\right|^2|\rho_{pn}^{(0)}\rangle \tag{B.25}$$

Solving with [41]:

$$\begin{aligned}|t_3\rangle =&\frac{1}{2}\sum_{m\neq 0}^{\infty}\sum_{k\neq 0}^{\infty}\left(-\frac{\mu^2}{2k+m}\right)^2\left(\frac{2k!}{\mu^2\Gamma(m+k+1)}\right)\left(\frac{2^{\frac{3}{2}}}{\mu^3}\right)\\ &\times\left|\alpha\mu^4\frac{\Gamma(\frac{m}{2}+3)\Gamma(m+k+1)}{k!\Gamma(m+1)}{}_2F_1\left(-k,\frac{m}{2}+3;m+1;1\right)\right.\\ &\left.+\beta\mu^6\frac{\Gamma(\frac{m}{2}+4)\Gamma(m+k+1)}{k!\Gamma(m+1)}{}_2F_1\left(-k,\frac{m}{2}+4;m+1;1\right)\right|^2|\rho_{pn}^{(0)}\rangle\end{aligned} \tag{B.26}$$

With each term being defined in Eq. (B.2), a sum over k with $m = 0$ yields the following result:

$$\begin{aligned}\rho_{00} =&\frac{\sqrt{2}}{\mu}Ae^{-\frac{r^2}{2\mu^2}}\\ &\times\left[1+\alpha\left(3\mu^4-2\mu^2r^2-\frac{r^4}{2}+\beta\left(-\frac{95\mu^{10}}{3}-40\mu^8r^2-4\mu^6r^4-\frac{2\mu^4r^6}{9}\right)\right)\right.\\ &+\beta\left(11\mu^6-6\mu^4r^2-\frac{3\mu^2}{2}r^4-\frac{1}{3}r^6\right)+\alpha^2\left(-\frac{3\mu^8}{2}-6\mu^6r^2-\frac{\mu^4}{2}r^4\right)\\ &\left.+\beta^2\left(-\frac{239\mu^{12}}{2}-66\mu^{10}r^2-\frac{15\mu^8}{2}r^4-\frac{2\mu^6}{3}r^6\right)\right]\end{aligned} \tag{B.27}$$

APPENDIX C: PERTURBED FIRST EXCITED STATE

Similarly to the fundamental case, the solution to Eq. (3.9) is given by Eq. (B.2), with perturbation (B.1). This time the focus is the case $k = 0$ and $m = 1$.

0^{th} order approximation to the first excited state

Refering to (3.10) with $k = 0$ and $m = 1$:

$$\rho_{01}^{(0)} = \sqrt{\frac{2}{\mu^2}} \left(\frac{r^2}{\mu^2}\right)^{\frac{1}{2}} e^{-\frac{r^2}{2\mu^2}}. \tag{C.1}$$

1^{st} order approximation to the first excited state

Starting form Eq. (B.5) with $p = 0$ and $n = 1$:

$$\begin{aligned} |\rho_{01}^{(0)}\rangle = &\sum_{m\neq 1}^{\infty}\sum_{k\neq 0}^{\infty} \left(-\frac{\mu^2}{2k+m-1}\right)\left(\frac{2k!}{\mu^2\Gamma(m+k+1)}\right)\sqrt{\frac{2}{\mu^2}} \\ &\times \int x^{\frac{m+1}{2}} e^{-x} L_k^m(x) \left[\alpha\mu^4 x^2 + \beta\mu^6 x^3\right] dx\, |\rho_{km}^{(0)}\rangle \end{aligned} \tag{C.2}$$

Next step:

$$\begin{aligned} |\rho_{01}^{(0)}\rangle = &\sum_{m\neq 1}^{\infty}\sum_{k\neq 0}^{\infty} \left(-\frac{1}{2k+m-1}\right)\left(\frac{2k!}{\Gamma(m+k+1)}\right)\frac{\sqrt{2}}{\mu} \\ &\times \left[\alpha\mu^4 \int x^{\frac{m+1}{2}+2} e^{-x} L_k^m(x) dx + \beta\mu^6 \int x^{\frac{m+1}{2}+3} e^{-x} L_k^m(x) dx\right] |\rho_{km}^{(0)}\rangle \end{aligned} \tag{C.3}$$

$$
\begin{aligned}
|\rho_{01}^{(0)}\rangle = &\sum_{m\neq 1}^{\infty}\sum_{k\neq 0}^{\infty}\left(-\frac{2}{2k+m-1}\right)\frac{\sqrt{2}}{\mu} \\
&\times\left[\alpha\mu^4\frac{\Gamma(\frac{m+1}{2}+3)}{\Gamma(m+1)}{}_2F_1\left(-k,\frac{m+1}{2}+3;m+1;1\right)\right. \\
&\left.+\beta\mu^6\frac{\Gamma(\frac{m+1}{2}+4)}{\Gamma(m+1)}{}_2F_1\left(-k,\frac{m+1}{2}+4;m+1;1\right)\right]|\rho_{km}^{(0)}\rangle
\end{aligned}
\tag{C.4}
$$

2^{nd} order approximation to the first excited state

$$
\begin{aligned}
|t_1\rangle = &\sum_{k\neq 0}\sum_{m\neq 0}\sum_{q\neq 0}\sum_{s\neq 0}\left(-\frac{\mu^2}{2k+m-1}\right)\left(-\frac{\mu^2}{2q+s-1}\right) \\
&\times\left(\frac{2k!}{\mu^2\Gamma(m+k+1)}\right)\left(\frac{2q!}{\mu^2\Gamma(s+q+1)}\right) \\
&\times\sqrt{\frac{2}{\mu^2}}\int x^{\frac{m+s}{2}}e^{-x}L_k^m(x)L_q^s(x)\left[\alpha\mu^4x^2+\beta\mu^6x^3\right]dx \\
&\times\int x^{\frac{q+s}{2}}e^{-x}L_q^s(x)\left[\alpha\mu^4x^2+\beta\mu^6x^3\right]dx\,|\rho_{km}^{(0)}\rangle
\end{aligned}
\tag{C.5}
$$

The same integrals from Appendix B are present, so t_1 is zero. For t_2:

$$
\begin{aligned}
|t_2\rangle = &\sum_{k\neq 0}\sum_{m\neq 1}\left(-\frac{\mu^2}{2k+m-1}\right)^2\left(\frac{2k!}{\mu^2\Gamma(m+k+1)}\right) \\
&\times\left(\frac{2}{\mu^2}\right)^{\frac{3}{2}}\int x^{\frac{m+1}{2}}e^{-x}L_k^m(x)\left[\alpha\mu^4x^2+\beta\mu^6x^3\right]dx \\
&\times\int xe^{-x}\left[\alpha\mu^4x^2+\beta\mu^6x^3\right]dx\,|\rho_{km}^{(0)}\rangle
\end{aligned}
\tag{C.6}
$$

$$
\begin{aligned}
|t_2\rangle = &\sum_{k\neq 0}\sum_{m\neq 1}\left(-\frac{\mu^2}{2k+m-1}\right)^2\left(\frac{2k!}{\mu^2\Gamma(m+k+1)}\right)\left(\frac{2}{\mu^2}\right)^{\frac{3}{2}} \\
&\times\left[\alpha\mu^4\int x^{\frac{m+1}{2}+2}e^{-x}L_k^m(x)dx+\beta\mu^6\int x^{\frac{m+1}{2}+3}e^{-x}L_k^m(x)dx\right] \\
&\times\left[\alpha\mu^4\int e^{-x}x^3dx+\beta\mu^6\int e^{-x}x^4dx\right]|\rho_{km}^{(0)}\rangle
\end{aligned}
\tag{C.7}
$$

$$
\begin{aligned}
|t_2\rangle =& \sum_{k\neq 0}\sum_{m\neq 1}\left(-\frac{\mu^2}{2k+m-1}\right)^2\left(\frac{2k!}{\mu^2\Gamma(m+k+1)}\right)\left(\frac{2}{\mu^2}\right)^{\frac{3}{2}} \\
&\times\left[\alpha\mu^4\int x^{\frac{m+1}{2}+2}e^{-x}L_k^m(x)dx+\beta\mu^6\int x^{\frac{m+1}{2}+3}e^{-x}L_k^m(x)dx\right] \\
&\times\left[6\alpha\mu^4+24\beta\mu^6\right]|\rho_{km}^{(0)}\rangle
\end{aligned}
\tag{C.8}
$$

$$
\begin{aligned}
|t_2\rangle =& \sum_{k\neq 0}\sum_{m\neq 1}\left(-\frac{\mu^2}{2k+m-1}\right)^2\left(\frac{2}{\mu^2}\right)\left(\frac{2}{\mu^2}\right)^{\frac{3}{2}} \\
&\times\left[\alpha\mu^4\frac{\Gamma(\frac{m+1}{2}+3)}{\Gamma(m+1)}{}_2F_1\left(-k,\frac{m+1}{2}+3;m+1;1\right)\right. \\
&\left.+\beta\mu^6\frac{\Gamma(\frac{m+1}{2}+4)}{\Gamma(m+1)}{}_2F_1\left(-k,\frac{m+1}{2}+4;m+1;1\right)\right] \\
&\times\left[6\alpha\mu^4+24\beta\mu^6\right]|\rho_{km}^{(0)}\rangle
\end{aligned}
\tag{C.9}
$$

For the last term:

$$
\begin{aligned}
|t_3\rangle =& \frac{1}{2}\sum_{m\neq n}^{\infty}\sum_{k\neq p}^{\infty}\left(\frac{\mu^2}{2(p-k)+n-m}\right)^2\left(\frac{2k!}{\mu^2\Gamma(m+k+1)}\right)\left(\frac{2p!}{\mu^2\Gamma(n+p+1)}\right)^{\frac{3}{2}} \\
&\times\left|\int x^{\frac{m+n}{2}}e^{-x}L_k^m(x)L_p^n(x)\left[\alpha\mu^4x^2+\beta\mu^6x^3\right]dx\right|^2|\rho_{pn}^{(0)}\rangle
\end{aligned}
\tag{C.10}
$$

First excited state $p=0$, $n=1$:

$$
\begin{aligned}
|t_3\rangle =& \frac{1}{2}\sum_{k\neq 0}^{\infty}\sum_{m\neq 1}^{\infty}\left(-\frac{\mu^2}{2k+m-1}\right)^2\left(\frac{2k!}{\mu^2\Gamma(m+k+1)}\right)\left(\frac{2}{\mu^2}\right)^{\frac{3}{2}} \\
&\times\left|\int x^{\frac{m+1}{2}}e^{-x}L_k^m(x)\left[\alpha\mu^4x^2+\beta\mu^6x^3\right]dx\right|^2|\rho_{pn}^{(0)}\rangle
\end{aligned}
\tag{C.11}
$$

$$
\begin{aligned}
|t_3\rangle =& \frac{1}{2}\sum_{k\neq 0}^{\infty}\sum_{m\neq 1}^{\infty}\left(-\frac{\mu^2}{2k+m-1}\right)^2\left(\frac{2k!}{\mu^2\Gamma(m+k+1)}\right)\left(\frac{2}{\mu^2}\right)^{\frac{3}{2}} \\
&\times\left|\alpha\mu^4\int x^{\frac{m+1}{2}+2}e^{-x}L_k^m(x)dx+\beta\mu^6\int x^{\frac{m+1}{2}+3}e^{-x}L_k^m(x)dx\right|^2|\rho_{pn}^{(0)}\rangle
\end{aligned}
\tag{C.12}
$$

$$
\begin{aligned}
|t_3\rangle =& \sum_{k\neq 0}\sum_{m\neq 1}\left(-\frac{\mu^2}{2k+m-1}\right)^2\left(\frac{2k!}{\mu^2\Gamma(m+k+1)}\right)\left(\frac{2}{\mu^2}\right)^{\frac{3}{2}} \\
&\times\left|\alpha\mu^4\frac{\Gamma(\frac{m+1}{2}+3)\Gamma(m+k+1)}{k!\Gamma(m+1)}{}_2F_1\left(-k,\frac{m+1}{2}+3;m+1;1\right)\right. \\
&\left.+\,\beta\mu^6\frac{\Gamma(\frac{m+1}{2}+4)\Gamma(m+k+1)}{k!\Gamma(m+1)}{}_2F_1\left(-k,\frac{m+1}{2}+4;m+1;1\right)\right|^2|\rho_{pn}^{(0)}\rangle
\end{aligned}
\tag{C.13}
$$

A summation with $m=1$ and a sum over k yields the following result:

$$
\begin{aligned}
\rho_{01} =& \frac{\sqrt{2}}{\mu}Ae^{-\frac{r^2}{2\mu^2}}\sqrt{\frac{r^2}{\mu^2}}\left[1+\alpha\left(9\mu^4-3\mu^2r^2-\frac{1}{2}r^4\right.\right. \\
&\left.+\,\beta\left(124\mu^{10}-240\mu^8r^2-16\mu^6r^4-\frac{2\mu^4}{3}r^6\right)\right) \\
&+\beta\left(44\mu^6-12\mu^4r^2-2\mu^2r^4-\frac{1}{3}r^6\right)+\alpha^2\left(\frac{51\mu^8}{2}-27\mu^6r^2-\frac{3\mu^4}{2}\right) \\
&\left.+\,\beta^2\left(-160\mu^{12}-528\mu^{10}r^2-40\mu^8r^4-\frac{8\mu^6}{3}r^6\right)\right].
\end{aligned}
\tag{C.14}
$$

APPENDIX D: FIXED POINT METHOD

The definitions given by (3.3) and (3.8) are used with a fixed point method to obtain the values of the coefficients A, α and β by fixing the value of μ. Defining U as

$$U(\alpha, \beta, r) = \frac{V(A, \alpha, \beta, r)}{A^2}, \tag{D.1}$$

allows to seed values α_0 and β_0 and get a new group (A_1, α_1, β_1).

$$A_1 = \sqrt{\frac{1}{\mu^4 U^{(2)}(\alpha_0, \beta_0, 0)}} \tag{D.2}$$

$$\alpha_1 = \frac{1}{4!} A_1^2 U^{(4)}(\alpha_0, \beta_0, 0) \tag{D.3}$$

$$\beta_1 = \frac{1}{6!} A_1^2 U^{(6)}(\alpha_0, \beta_0, 0) \tag{D.4}$$

These new values are seeded to get (A_2, α_2, β_2), (A_3, α_3, β_3) and so on until convergence is reached.